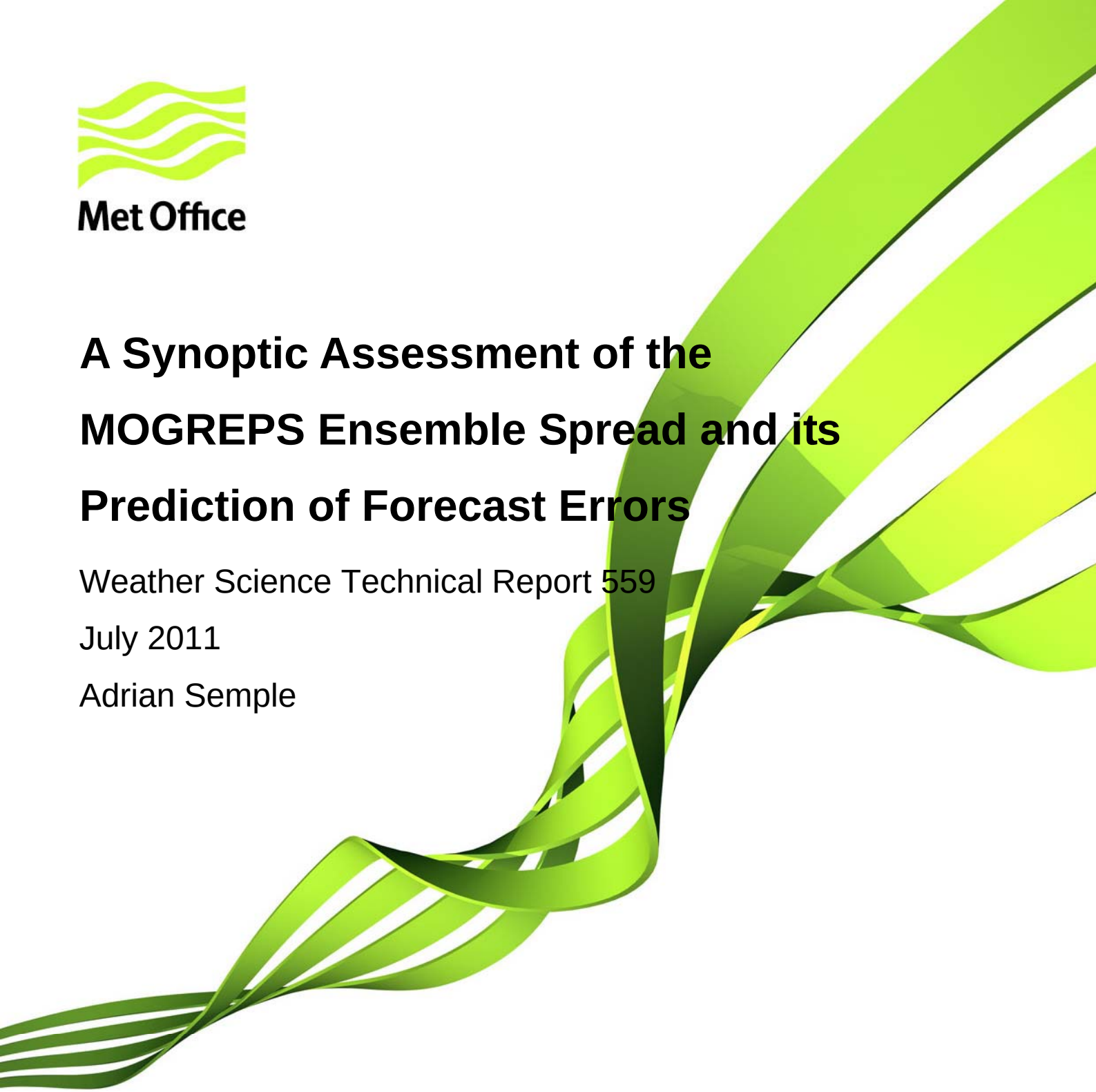

A Synoptic Assessment of the MOGREPS Ensemble Spread and its Prediction of Forecast Errors

Weather Science Technical Report 559

July 2011

Adrian Semple

Contents

1. Introduction 3

2. Ensemble Mean & RMS Errors 5

Ensemble Mean 5

Ensemble RMS Error 5

3. Ensemble Spread 7

Ensemble Standard Deviation and GM Error 7

Ensemble Standard Deviation and Ensemble RMS Error 9

4. Summary and Conclusions 11

5. Acknowledgments 12

6. References 13

Abstract

The primary aim of the MOGREPS ensemble system is to provide a means of evaluating the uncertainty in a forecast with a priori information. The uncertainty of the forecast is reflected in the spread of the 24 member ensemble in which each member is run from an analysis perturbed from that of the control member. This paper considers the MOGREPS ensemble from within a dynamical meteorology framework and compares the performance of the ensemble with that of the deterministic Global Model (GM). It is illustrated through the use of ‘error-tracking’ techniques that the ensemble provides a reasonable representation of the dynamically active regions and suggests a relatively successful determination of the sensitive areas with an improvement over earlier MOGREPS versions. It is also shown that the forecast errors of the ensemble are consistent with those of the high resolution GM suggesting no unintentional modelling errors have been introduced as a result of the ensemble process. It is then demonstrated that the spread of the ensemble is a good indicator of areas of developing unpredictability in the forecast but uses Hovmöller analysis techniques to show that the ensemble is significantly under-dispersive across the dynamically active midlatitude regions. It is concluded that there appears to be no systematic focus to the under-dispersive nature of the ensemble but that the ensemble generally under-represents the forecast error by a factor of ~2. This has the effect that the under-representation of the error within areas of increasingly high dynamical activity - and by inference challenging forecasting situations - becomes increasingly evident.

1. Introduction

Unpredictability is inherently linked to dynamically active areas. These areas represent the regions of the atmosphere which are unstable, often rapidly growing, and are thus characterized by being highly sensitive to errors in the initial state.

A sequence of Global Model (GM) analyses of certain key meteorological fields can be used to identify the probable location of these areas by an understanding of the dynamics involved in energetic developments. Figure 1 shows GM fields for 850hPa θ_w, MSLP, 250hPa gph and 250hPa wind speed for 28th April 2011. Together with an upper vorticity field, these diagnostics can help cover many of the important mechanisms involved in meteorological developments and be used to infer where growing states and sensitivity to initial conditions are likely to occur. For example, a strong thermal gradient near the dynamically-active exit of an upper jet accompanied by vorticity advection from a driving upper trough could all be contributors to strong growth, and one would expect some correlation between this and sensitive areas. Also shown in Figure 1 are the MOGREPS T+0 spread of 500hPa gph and the ECMWF RMS of the 500hPa singular vector (SV) perturbations, both of which represent diagnosed uncertainties of their respective ensembles. One can use the meteorological fields to notice instances of agreement between the dynamically-inferred sensitive areas and those areas of uncertainty arrived at by the system of the relevant ensemble. The sharpening major upper trough and associated strong thermal gradient and developing surface depression in the Great Lakes area of the USA, for example, has been identified by both of the ensemble methods as a particularly sensitive area at this time.

Investigations of forecast errors by the author using error tracking techniques have shown clear evidence of the relationship between dynamically-active areas and sensitive areas diagnosed as part of an ensemble system. Errors detected at long ranges can be traced back through the forecast with techniques such as forecast-analysis differences to uncover the geographical and temporal origins of a forecast error. Figure 2 shows the 250hPa gph error tracking (forecast-analysis) for the QG00 28th April 2011 forecast. The results show the dynamical developments which have successively been predicted poorly since the start of the forecast and their effects on downstream developments as the forecast evolves. Often such techniques show multiple error sources which interact

over the course of the forecast to contribute to the overall error. In most cases, these error sources can be associated with specific dynamical developments which for some reason have been misrepresented in the initial conditions. In this case the primary error sources of the Northern Hemisphere are identifiable as those in the western North Pacific (identified by the positive and negative wave-train at T+24) and North America (this arrived at by extrapolating back the location of the error at T+24 to allow for its propagation since T+0). On this basis, the error tracking can be used to validate the sensitive area prediction methods, and in this case reasonably good agreement is observed between all methods (compare Figure 1 and Figure 2). This is not always the case however.

Reasons for analysis error can be varied, such as model error, the assimilation of poor observations, or problems with the assimilation system or the observation quality control. It is also possible that the error has occurred as a result of the statistical nature of the assimilation process in which ‘good’ observations result in analysis increments which (by random) incorrectly project onto a rapidly growing state (discussed in Semple 2011).
The aim of ensemble forecasting is to provide a priori information about the quality of an NWP forecast by giving a measure of the uncertainty in a forecast – the uncertainty largely arising from the problems arising from determining the initial conditions. This is achieved by perturbing the initial conditions (i.e. the best analysis) and by observing the impact on the spread within the resulting forecasts; the ensemble spread also indicating the scope of alternative dynamical developments and their respective likelihood.
It is also now recognised that a significant contribution to forecast uncertainty arises from a need to take account of model error. This originates from a number of sources such as unrepresented subgrid-scale processes or from parameterization uncertainties. Stochastic physics schemes, in particular, are now being employed in order to represent the statistical aspects of the processes in the driving deterministic model which may be improperly represented.

Irrespective of the error source, the ensemble spread is related to the forecast uncertainty – low spread indicating low uncertainty and large spread indicating high uncertainty. At the verification time the ensemble spread reflect the likely magnitude of the forecast error.

This report looks at an assessment of the MOGREPS ensemble by considering how effectively the spread of the ensemble predicts forecast error. For these purposes, the discussion will consider the larger scale synoptic flow of 500hPa gph, since this is a

good overall representative field on which to base the study. The results presented in the report are drawn from a daily assessment of cases made during April to June 2011.

2. Ensemble Mean & RMS Errors

Ensemble Mean

The ensemble mean is obtained by averaging the forecasts from all the ensemble members. Figure 3 and Figure 4 shows a comparison of the ensemble mean error and GM error at a constant verification time of 00UTC 20th April 2011 (i.e. a sequence of six successive forecasts with forecast lead times T+12 to T+72 verifying at the same time). The figures clearly show a strong relationship between the ensemble mean error and GM error with errors of similar magnitude occurring in the corresponding areas of the fields. This is as one would hope since the ensemble is based on the same Global Model ran at lower resolution.

The ensemble mean necessarily produces a field which is smoother than the deterministic forecast not only because of the lower resolution of the ensemble but because the spread of the ensemble will produce a smoother field: regions of high spread leading to smoother fields. Within this context, the ensemble mean effectively filters out the unpredictable elements of the forecast. This effect can be observed in the cut-off vortex to the west of Spain – at shorter lead times the vortex appears similar in both the GM and ensemble mean, but as the forecast range evolves a clearly more bland field appears in the ensemble compared with that of the GM. This is an indication of the high uncertainty (and therefore high spread) in the development of this feature as the forecast progresses.

Ensemble RMS Error

It is more interesting to compare the root-mean-square (RMS) error of the ensemble with the GM error as this is observed to better highlight the synoptic-dependent features within the ensemble which are smoothed out by the ensemble mean.

Figure 5 and Figure 6 show a comparison of the 500hPa gph RMS error of the MOGREPS ensemble and GM error for a verification time 00UTC 30th April 2011 (i.e. individual successive forecasts verifying at the same time, ten days after the comparison of Figure 3 and Figure 4). At short range the RMS error is clearly larger than that of the

GM, a result of the fact that the ensemble is composed of forecasts ran from analyses which are perturbed away from the best analysis from which the GM is run. With increasing forecast range both errors grow with the ensemble RMS error remaining noticeably larger than that of the GM error. As the forecast range extends it is clear that there is a relatively good correlation between the location of the error maxima in the ensemble and in the GM. The maxima in both cases are observed to occur within the dynamically-active areas of the major upper troughs with larger errors occurring where instability is likely to be largest – i.e. in the sharper, more vigorous features and in those areas which have recently undergone trough extensions leading to vortex development. This suggest that the perturbations of the ensemble members are providing a reasonable indication of unpredictable developments in the subsequent forecasts.

Analysing these fields over a long period is a useful method of determining the robustness of the ensemble RMS Error and GM error relationship. This has been done by both direct use of the shown charts but also by the calculation of Hovmöller diagrams. Hovmöller diagrams have the benefit of averaging the signal over a latitudinal band thereby helping to highlight the larger scale signal, and because they are a function of time, by more clearly disclosing the consistency of the signal. For these purposes, the GM RMS error has been calculated (rather than the absolute GM error shown in Figure 5 and Figure 6) to preserve the signal when the mean of the (RMS) error is calculated over the latitudinal band of the Hovmöller diagram.

Figure 7, Figure 8 and Figure 9 show a comparison of calculated Hovmöller diagrams of the ensemble 500hPa gph RMS error and GM RMS errors for forecast ranges T+24, T+48 and T+72 respectively for a period ~1 week. The Hovmöller diagrams have been calculated by averaging the RMS errors across latitudes 40-70N to coincide with the maximum of the midlatitude dynamical activity. At short-range, the MOGREPS RMS error is clearly larger than that of the GM for reasons already discussed. However, even at this range it is clear that there is a correlation between the areas in which the GM RMS errors occur and those areas identified within the ensemble. For example, the structures running diagonally down the GM RMS errors from top-left to bottom-right at T+24 are already identifiable as the most intense structures within the MOGREPS RMS errors, indicating a relatively successful perturbation of the sensitive dynamical areas. The correlation then continues through the forecast range to T+72 where the RMS error of the ensemble may be up to twice the magnitude of the GM. The error structures at 30E, which are some of the largest GM errors of the period, are associated with the

largest ensemble RMS errors of the period. Other occurrences of large GM error such as that at 60W and 140E are well represented in the ensemble RMS error.

Figure 10 shows the MOGREPS RMS error and GM error at T+72 on the 7th May 2011 corresponding to a horizontal section of the Hovmöller diagrams of Figure 9. This shows that the maximum GM and ensemble error observed at 30E in the Hovmöller diagram is due to the handling of the upper vortex near the Black Sea. This has developed from a trough disruption during the preceding days and is a process that past model performance has shown to be inherently difficult to model with relatively low predictability. A large RMS error in this region associated with this feature is therefore entirely consistent with the aims of the ensemble. From this point of view, the same conclusions may be drawn about the features at 30W and 60W.

As discussed earlier, the larger magnitude of the ensemble RMS error compared with the GM RMS error reflects the fact that the ensemble members are being ran from perturbed analyses with perturbations of the order of magnitude of the analysis errors. This means that the ensemble members are in general of significantly lower skill than that of the control forecast, and also of the higher resolution Global Model.

The consistency of the ensemble RMS error and GM RMS error observed in this study is an important result. This ensures that the performance of the Global Model driving the two forecast systems is consistent, since inconsistency in their errors would suggest errors in the ensemble that have been introduced unintentionally. Also, the consistency shows that developments unrepresentative of any features which would develop in the high resolution Global Model are absent.

3. Ensemble Spread

Ensemble Standard Deviation and GM Error

The ensemble spread more directly reflects the sensitivity of the individual ensemble member forecasts to both uncertainties in the initial conditions and in the model, and by this relationship is generally used to attribute an a priori confidence to an NWP forecast. A forecast of low spread would generally be associated with a deterministic forecast which verifies well. A forecast of large spread will generally be associated with a deterministic forecast which is more likely to verify poorly, although it does not preclude

this and the deterministic forecast may in fact verify well (probabilities aside, the deterministic model is of a higher resolution and running from a superior analysis than the ensemble members).

Figure 11 and Figure 12 show a comparison of the ensemble spread and GM error for the QG00 27th April 2011 forecast (i.e. the development of the ensemble spread through a single forecast). Note that in this case the GM error is on a slightly reduced scale relative to that of the ensemble spread. The growth of the ensemble spread is quite rapid, with the dynamically active areas developing larger spread and quickly showing increased sensitivity to the initial perturbations. There is some correlation visible by T+36 between the ensemble spread and the GM error, but this is less clear than in the RMS error comparisons discussed earlier in which the association was more direct. Nevertheless, the largest errors at this forecast range occur again with the upper vortices over the North Atlantic, North America and western Pacific identified within the ensemble spread.

The trough in the North Atlantic undergoes a rapid extension in the following 36 hours, and extends southwards to beyond 40N by T+72. As discussed earlier, this process is common and difficult to model so that the relatively high spread evident in parts of the trough seems reasonable. The GM error at this time shows that the GM has performed relatively well in this particular case, although the trough has extended too far south on it's southern flank as indicated by the negative errors. In this instance the ensemble spread appears to have captured the GM error well.

In contrast, the GM error associated with the trough over Quebec is of a similar magnitude at T+72 and is too flat, but is relatively under-represented in the ensemble spread. Just upstream over central USA, an upper trough has incorrectly undergone trough disruption in the forecast and has progressed too slow eastwards as a result. Although there is some indication of higher ensemble spread in the area, the spread is probably too low relative to the size of the observed error.

Figure 13 and Figure 14 show the same comparison but for a constant verification time of 20th April 2011 (thus being six successive forecasts and of the same period as Figure 3 and Figure 4). Similar conclusions may be drawn from these forecasts, although in general the ensemble spread appears to be representing the GM errors well. Note that a comparison with Figure 3 and Figure 4 shows that the areas of larger ensemble mean error also appear well correlated with the areas of larger ensemble spread – particularly

the region to the north of the UK and the region to the west of Spain. Both these regions would be identified through an application of error tracking techniques and dynamical activity and suggest that the ensemble is providing a reasonably effective assessment of the situation.

Ensemble Standard Deviation and Ensemble RMS Error

Thus far the assessment of the MOGREPS ensemble has centred on a comparison of the ensemble with the high resolution deterministic model. This has proved useful in determining that the ensemble has a reasonable representation of the sensitive and dynamically active areas and that the forecasts from the ensemble are consistent with those of the high resolution GM. It has also shown that the ensemble error is considerably larger than that of the deterministic model as a result of running from perturbed analyses and that the spread appears to be reasonably well correlated with the errors of the deterministic model.

The spread of the ensemble is now assessed further since it is this quantity which provides the important information (confidence) on forecast errors in both the ensemble and by inference in the high resolution deterministic model. Figure 15 and Figure 16 show a comparison of the 500hPa gph ensemble spread with the ensemble RMS errors for the verification time 12UTC 10th May 2011. As already discussed the RMS error of the ensemble is a combined effect of the perturbed analyses on the forecasts which result in varied skill at the verification time. The ensemble spread is intended to be the a priori information on the RMS error and so one would aim for them to be closely correlated. Figure 15 and Figure 16 show that in the early part of the forecast (T+12) the ensemble spread is beginning to correctly increase in the regions which are associated with larger RMS error. Again, the dynamically active areas of the disrupting upper trough over the USA and the intense vortex over eastern China are rapidly identified and these appear as some of the larger errors in the RMS errors. This process continues as the forecast range increases, with the locations of the developing maxima in the ensemble spread reasonably well correlated with those of the RMS error at T+36. At this range, all the main dynamically active areas which verify poorly at the verification time have been identified by maxima in the ensemble spread. By T+72 it is clear that the ensemble spread has effectively identified the regions of large ensemble error, and that a reasonable correlation exists between the maximum locations identified.

Figure 17 shows calculated correlation statistics for the 500hPa gph spread and RMS error for the period ~1 week in the northern hemisphere. Although variability clearly exists, correlation coefficients are obtained typically ~0.45 for T+48 and ~0.55 for T+72. This appears to be reasonable when compared with similar comparisons of other ensemble systems (Grimit, 2007).

The comparison of Figure 15 and Figure 16, however, also highlights that although a reasonable correlation exists between the location of the maxima of the RMS error and ensemble spread, the ensemble spread under-represents the magnitude of the error by a factor of ~2. The under-dispersive nature of the ensemble is evident from the early forecast range (T+12), becoming obvious by T+48, and very significant by T+72. Specifically, at T+72 the areas of large dynamical activity are under-represented – for example the intense vortex over eastern China with an associated large RMS error shows only a modest indication of high spread in the ensemble whilst the disrupting upper trough over the USA suggests a much higher degree of predictability in the ensemble spread than inferred by the ensemble RMS error. There appears to be no systematic under-representation of any particular type of dynamical development, rather a more general lack of dispersion in the ensemble.

To address this further, Hovmöller diagrams have been calculated to compare the ensemble standard deviation with the ensemble RMS error and are shown in Figure 18, Figure 19 and Figure 20. As in Figure 7, Figure 8 and Figure 9, the Hovmöller diagrams have been calculated across a latitudinal band 40N-70N to coincide with the region of maximum dynamical activity. The figures show that at T+24 the mean ensemble spread identifies some of the errors which subsequently develop in the ensemble RMS errors, but that these are under-represented. Most structures within the RMS errors are clearly unidentifiable within the general spread of the ensemble.

At T+48 the structures within the ensemble RMS errors have become very clear, with high intensity features throughout the period at e.g. 30-60W and 120-180E. By their presence in the vertical of the error diagram these represent long-lived errors within the ensemble (and the GM, not shown) but which are heavily under-spread in the ensemble. The trend continues to T+72 in which the mean spread appears very bland relative to the mean RMS error.

Because the Hovmöller technique involves a mean across a range of latitudes, it is possible that the interpretation of the results may be heavily based on the chosen

latitude ranges. For example, a wider range of latitudes would necessarily produce a smoother field in both the RMS error and the ensemble spread and this may mask a better performance of the ensemble at high or lower latitudes. To verify the signal from the broad midlatitude ranges of the previous figures, the process was repeated dividing the latitudinal band of Figure 18, Figure 19 and Figure 20 into latitude ranges 30N-50N and 50N-70N with the results shown in Figure 21, Figure 22 and Figure 23 and Figure 24, Figure 25 and Figure 26 respectively.

The results show the majority of the RMS error within the range 30N-70N lies within the northern part of the latitudes. The performance of the ensemble is reasonably similar in both the north and the south although the intensity of the spread in the north is slightly suggestive of a marginally better relationship here. Nevertheless, these comparisons confirm the conclusion that the ensemble is heavily under-spread.

4. Summary and Conclusions

1. An application of dynamical meteorology and error tracking techniques have been used to validate the development of forecast spread within the ensemble. The ensemble has a reasonable representation of the dynamically active regions suggesting that the sensitive areas predicted by the ensemble are developing in areas consistent with dynamical meteorology. This is a very positive result which shows a great improvement from earlier versions of the MOGREPS ensemble system.
2. The forecasts from the ensemble are consistent with those of the high resolution GM suggesting that the observed increased RMS error of the members is a direct result of the perturbed analyses as intended and not as a result of an unintentional error introduced into the forecasts by the ensemble process.
3. The location of the developing maxima in the spread of the ensemble is reasonably well correlated with the location of the RMS error maxima providing useful a priori information about the level of unpredictability in the forecast. The correlation appears reasonably consistent with time.
4. The ensemble is significantly under-dispersive (by a factor ~2) across the dynamically active midlatitude regions suggesting further account is required of statistical aspects of model error.
5. There appears to be no systematic under-representation of particular meteorological developments, rather a general lack of dispersion within the ensemble. However,

areas of high dynamical activity such as vortices, sharpening upper troughs and trough disruptions are sites of significant development where the ensemble's under-dispersive nature is more clearly evident and so can limit its usefulness. Whilst a future increase in the resolution of the ensemble is likely to lead to a reduction in the observed RMS error of the ensemble members, past resolution upgrades have also shown a benefit in increased spread of the ensemble.

Modern data assimilation systems use a climatology of short-range forecast errors to provide a way of combining observations with the model background in order to produce an analysis. Such a climatological approach is limited because it provides no information on the synoptic error pattern which varies considerably from day to day. In July 2011, the Met Office implemented a 'hybrid' data assimilation system which provided a flow-dependent component derived from the MOGREPS ensemble to the existing 4D-Var assimilation techniques so as to improve on the short-range forecast errors.

For hybrid data assimilation the most important properties of the ensemble are (a) the distribution of the spread and (b) the correlation structures amongst the members (not studied in this report). The work documented in this report has shown that the dynamically active areas are reasonably well accounted for within the ensemble, and although there is an overall lack of spread, the distribution of the spread agrees well with the distribution of the errors from the GM. Thus, as far as the hybrid is concerned, the overall spread of the ensemble is adjusted within the hybrid system to meet certain tuning criteria, so that any lack of spread within the ensemble should not in fact be detrimental to the scheme's performance. Assuming the correlation structures are also sensible, one would expect the use of the ensemble data within the hybrid system to improve the representation of the background error covariances.

The positive results from trials of the hybrid system (~1% forecast skill improvement against observations) suggest that the representation of background errors has indeed been improved.

5. Acknowledgments

Thanks to Richard Swinbank, Warren Tennant, Rick Rawlins, Mike Thurlow and Adam Clayton for their discussion and comments.

6. References

Grimit, Eric P., Clifford F. Mass, 2007: Measuring the Ensemble Spread–Error Relationship with a Probabilistic Approach: Stochastic Ensemble Results. Mon. Wea. Rev., 135, 203–221

Semple A.T., M. Thurlow and S. Milton, 2011. Experimental Determination of Forecast Sensitivity and the Degradation of Forecasts Through the Assimilation of Good Quality Data. *Submitted to Mon. Wea. Rev.*

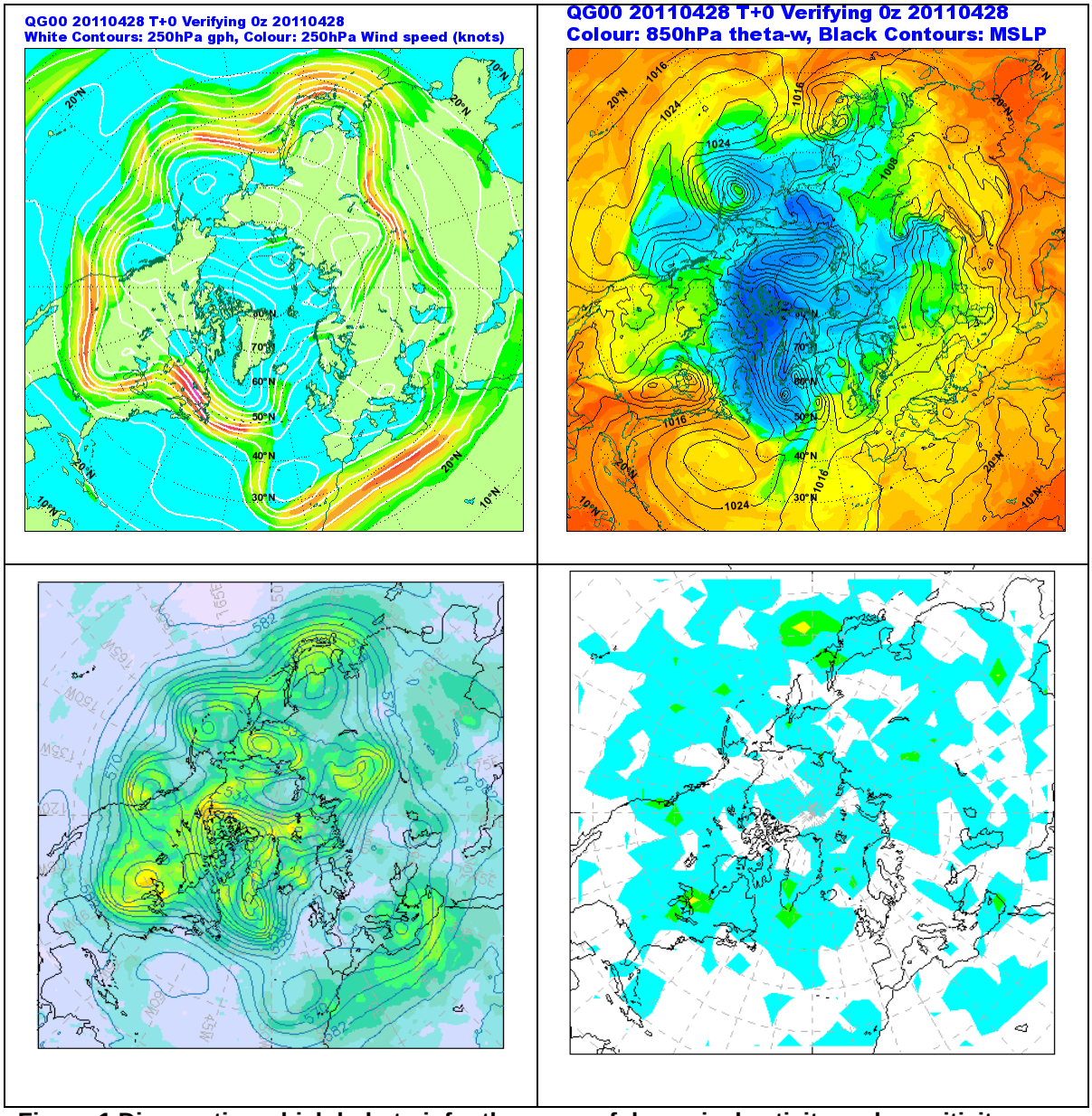

Figure 1 Diagnostics which help to infer the areas of dynamical activity and sensitivity. TOP LEFT : 250hPa wind (coloured field) with 250hPa gph (white contours). TOP RIGHT: 850hPa theta-w (coloured field) with MSLP (black contours). A vorticity field (relative/absolute/potential) is also typically used (not shown). LOWER LEFT: MOGREPS 500hPa gph T+0 spread at 00z 28th April 2011 and LOWER RIGHT: ECMWF RMS of the 500hPa perturbations at 00z 28th April 2011.

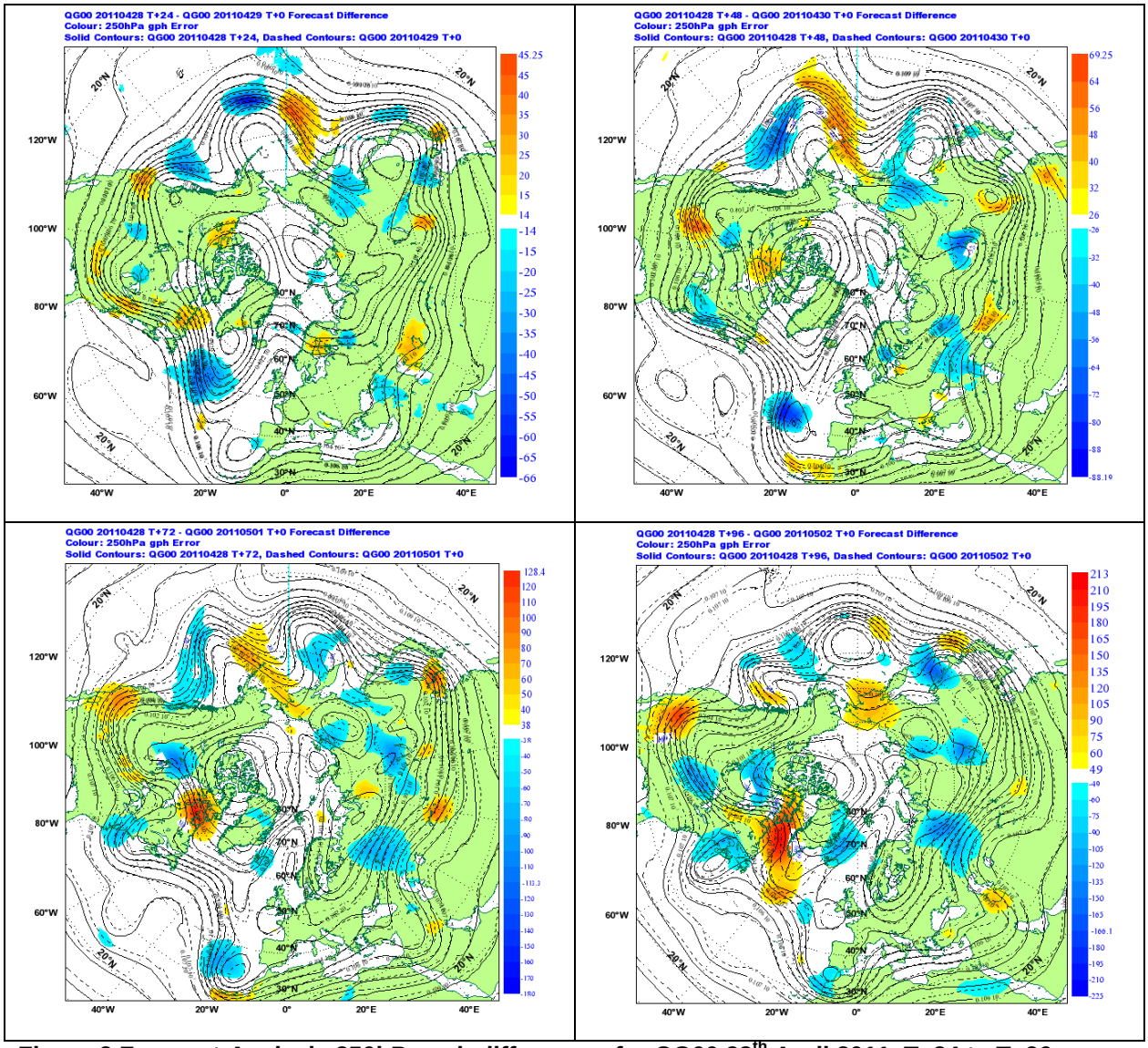

Figure 2 Forecast-Analysis 250hPa gph differences for QG00 28th April 2011, T+24 to T+96. The colours indicate the forecast error at each step which can be used to track the evolving errors of a forecast back to their origins. In this case the primary errors in the forecast originate over North America (appearing as the blue error in the North Atlantic at T+24) and in the western North Pacific (appearing as the blue and red wave-train at T+24). These errors and their downstream impacts can be followed through subsequent frames. Also shown, solid contours: forecast, dashed contours: analysis.

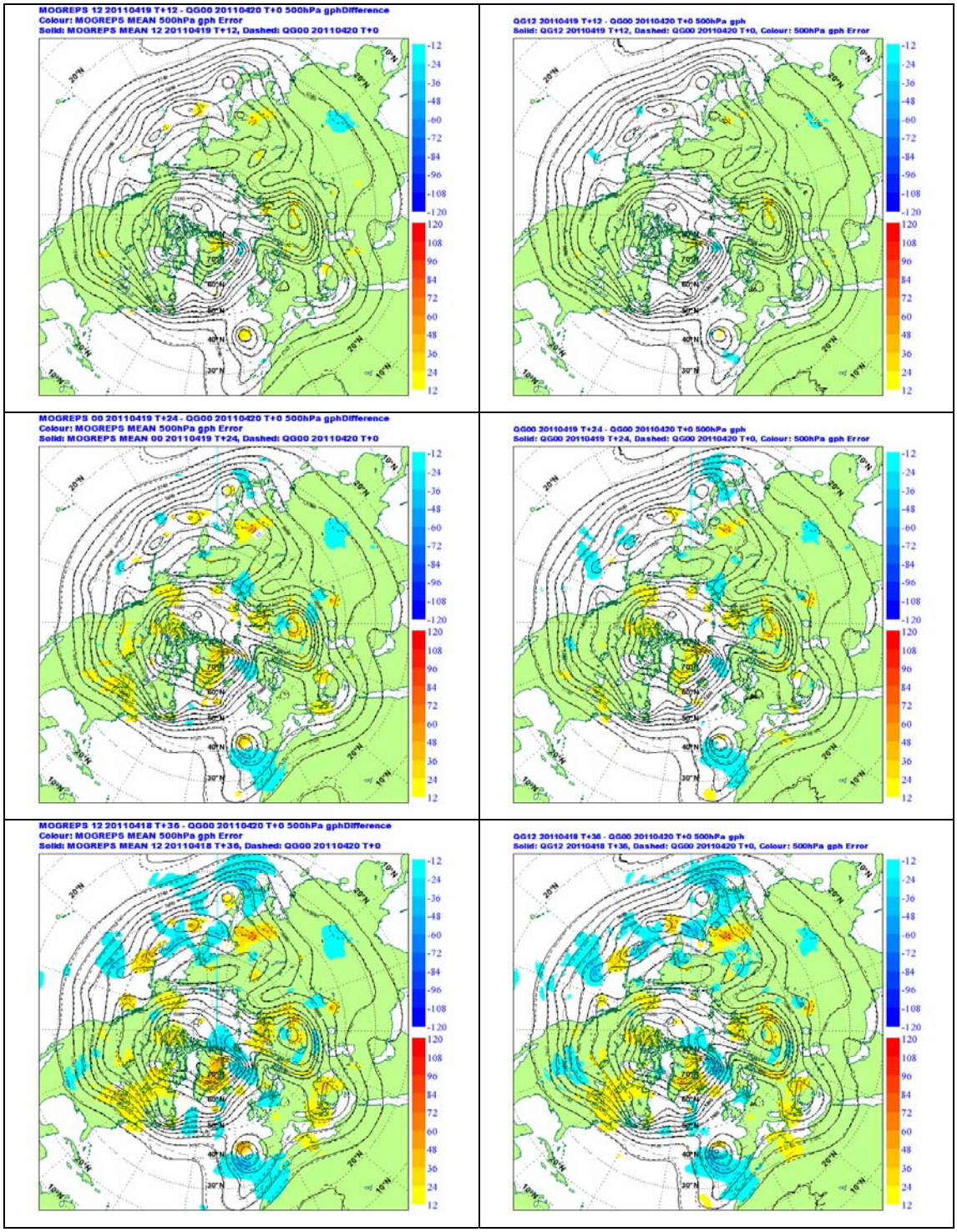

Figure 3 MOGREPS ensemble mean error (left) versus Global Model error (right), 500hPa gph T+12 to T+36 for the Northern Hemisphere with forecast *verification time* 00UTC 20th April 2011.

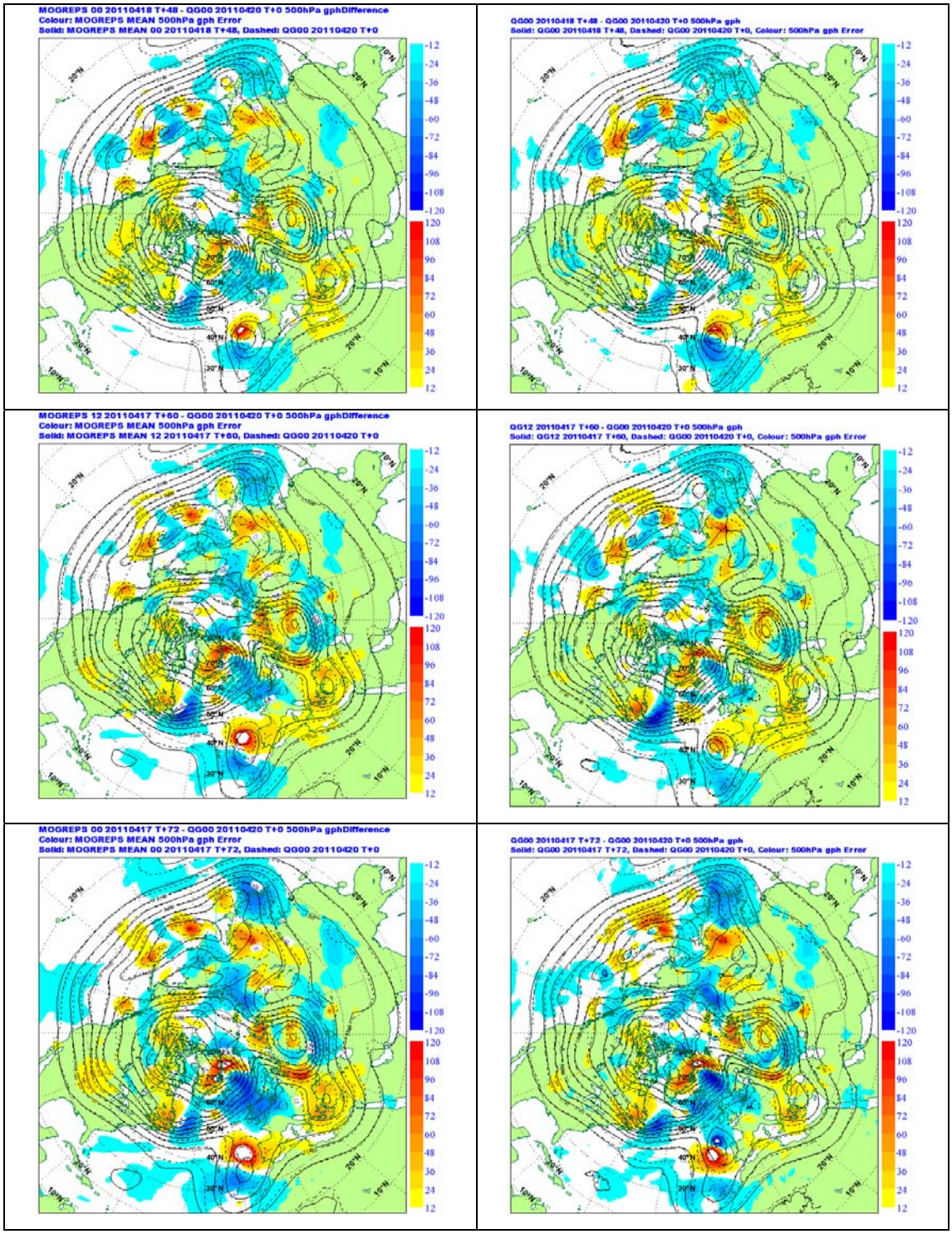

Figure 4 MOGREPS ensemble mean error (left) versus Global Model error (right), 500hPa gph T+48 to T+72 for the Northern Hemisphere with forecast *verification time* 00UTC 20th April 2011.

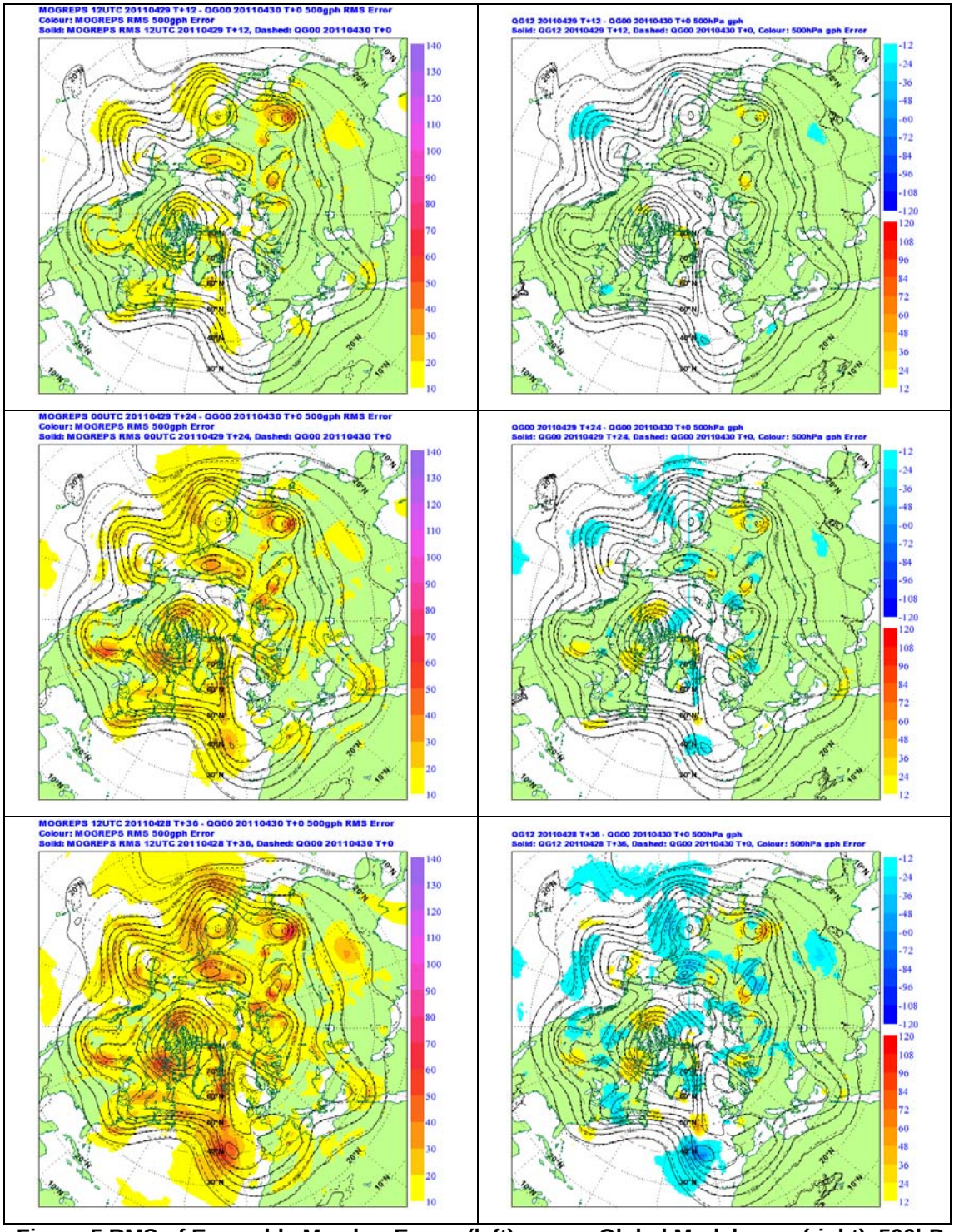

Figure 5 RMS of Ensemble Member Errors (left) versus Global Model error (right), 500hPa gph T+12 to T+36 for the Northern Hemisphere with forecast *verification time* 00UTC 30th April 2011.

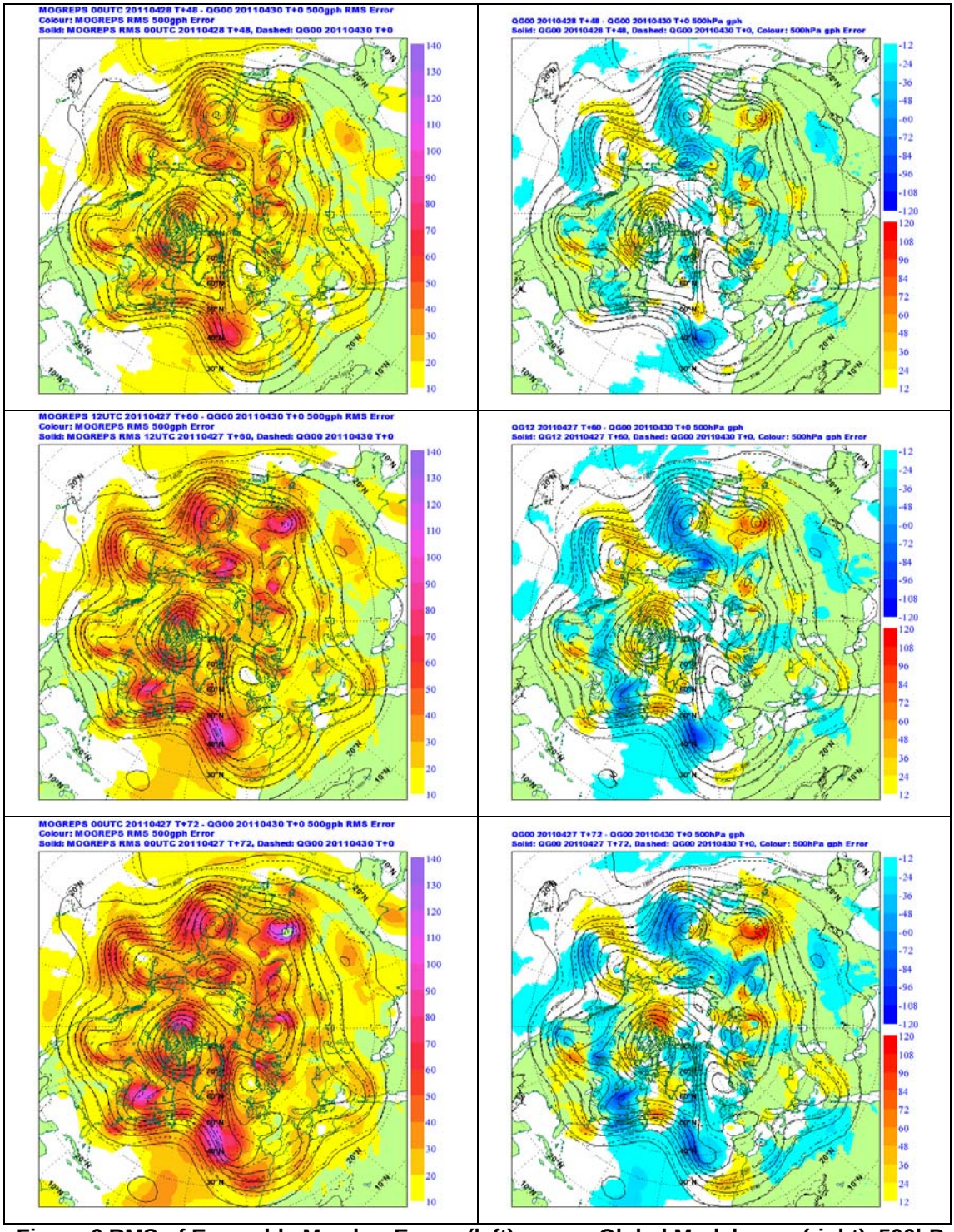

Figure 6 RMS of Ensemble Member Errors (left) versus Global Model error (right), 500hPa gph T+48 to T+72 for the Northern Hemisphere with forecast *verification time* 00UTC 30th April 2011.

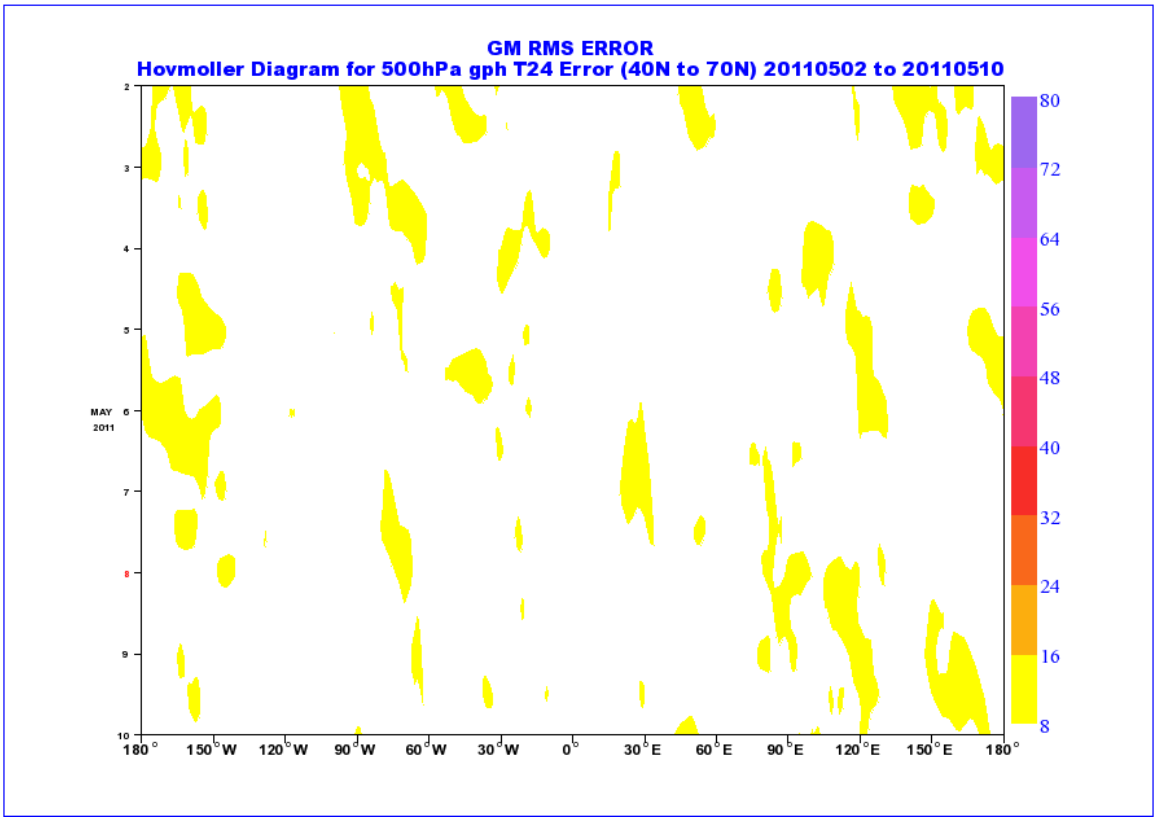

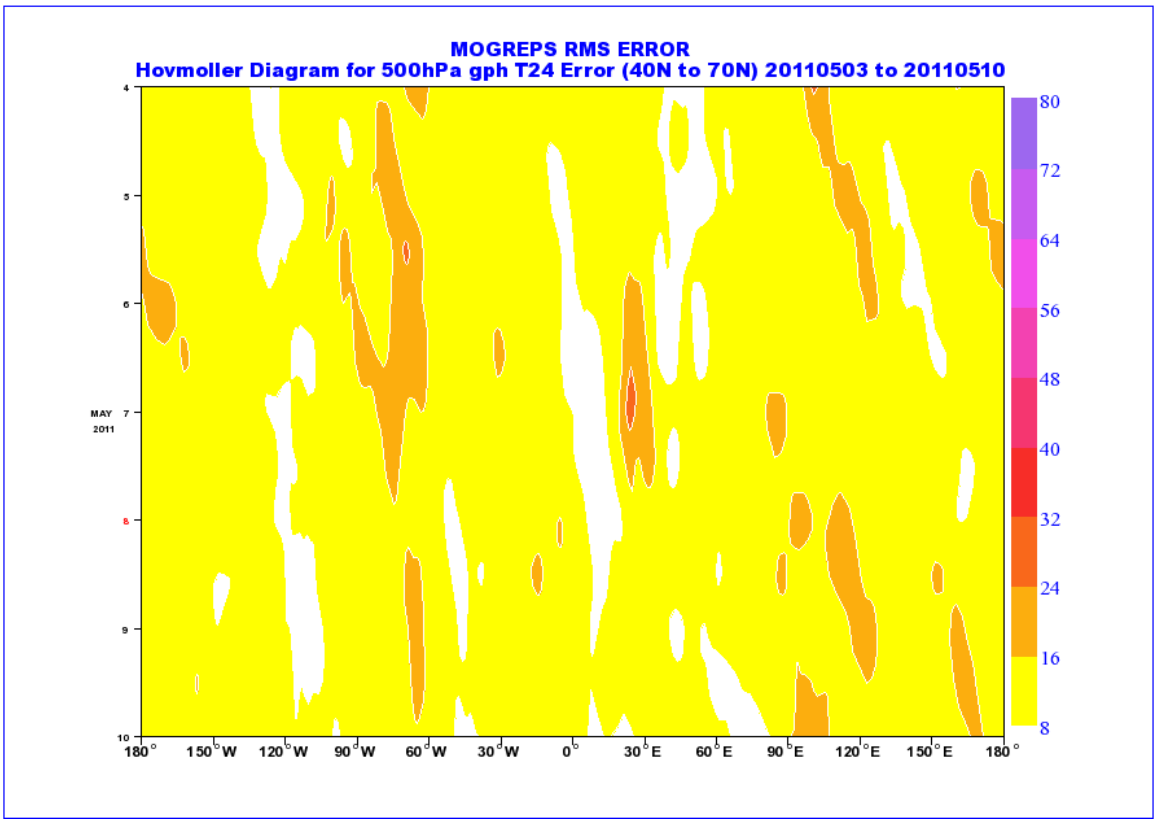

Figure 7 GM 500hPa gph Error versus Ensemble RMS Error, T+24.

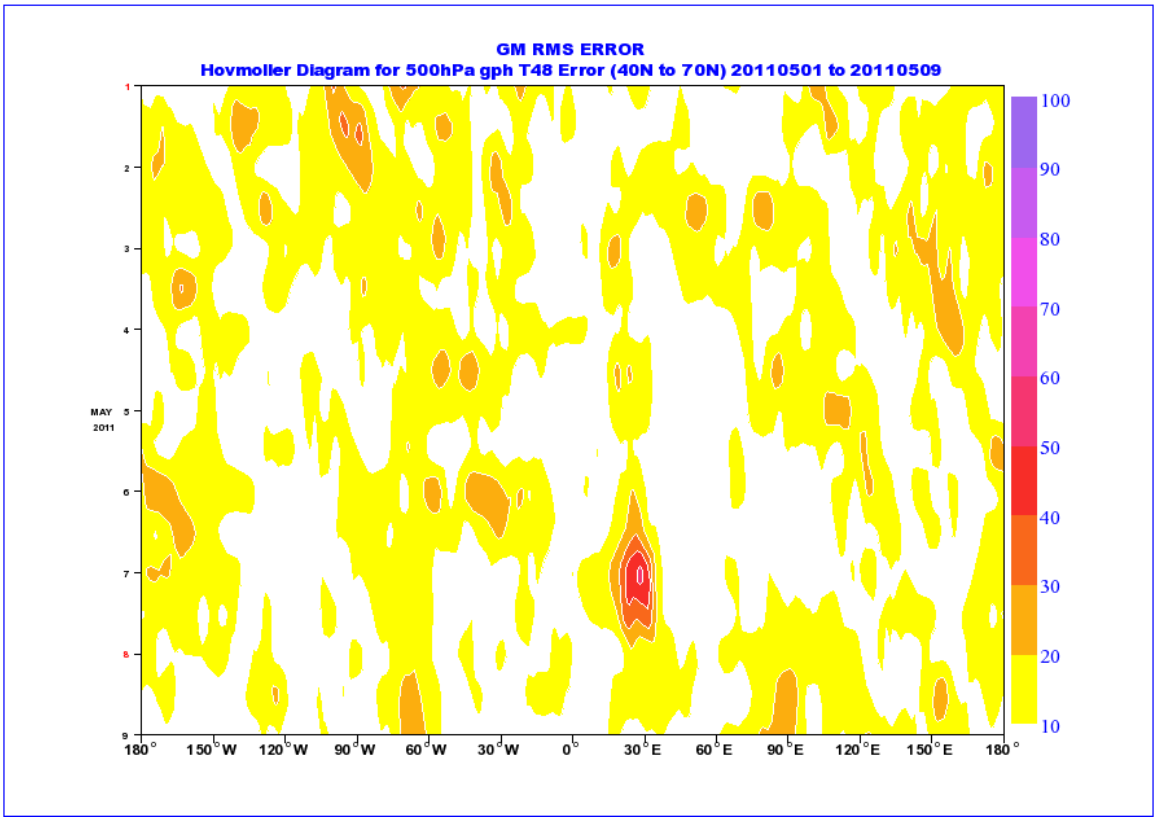

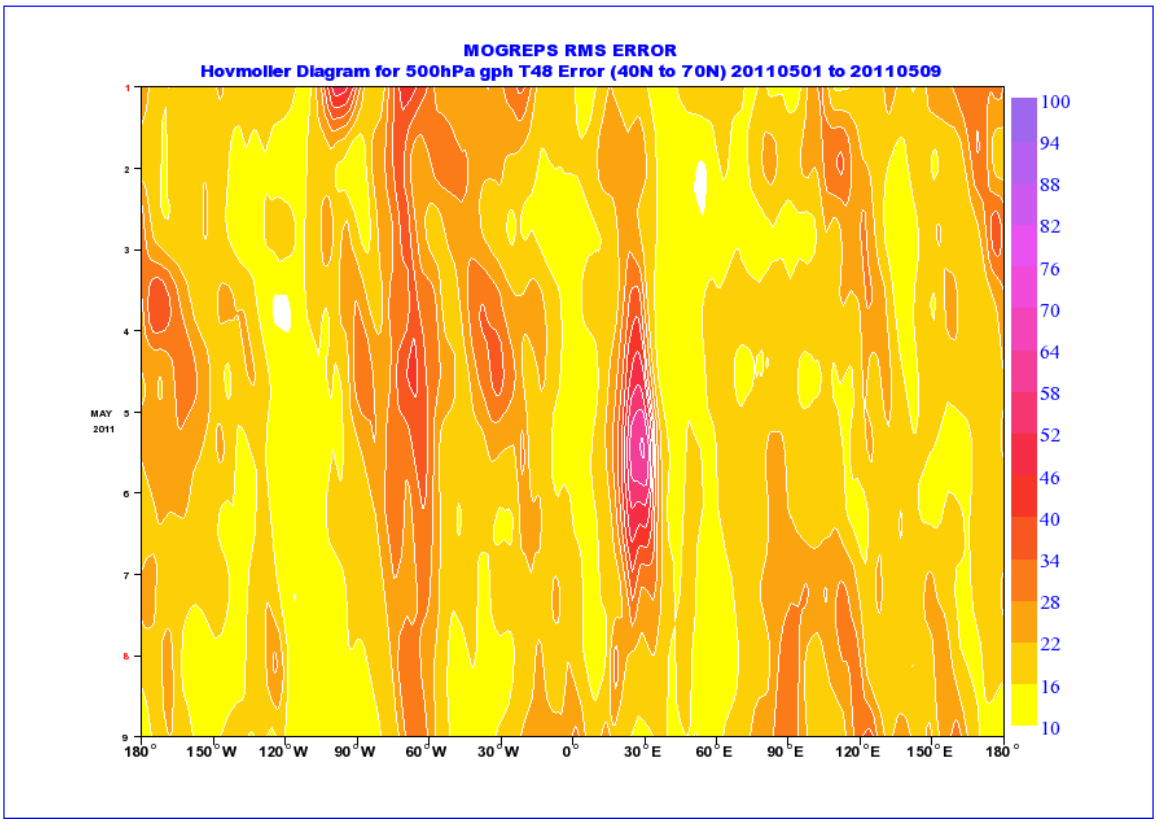

Figure 8 GM 500hPa gph Error versus Ensemble RMS Error, T+48.

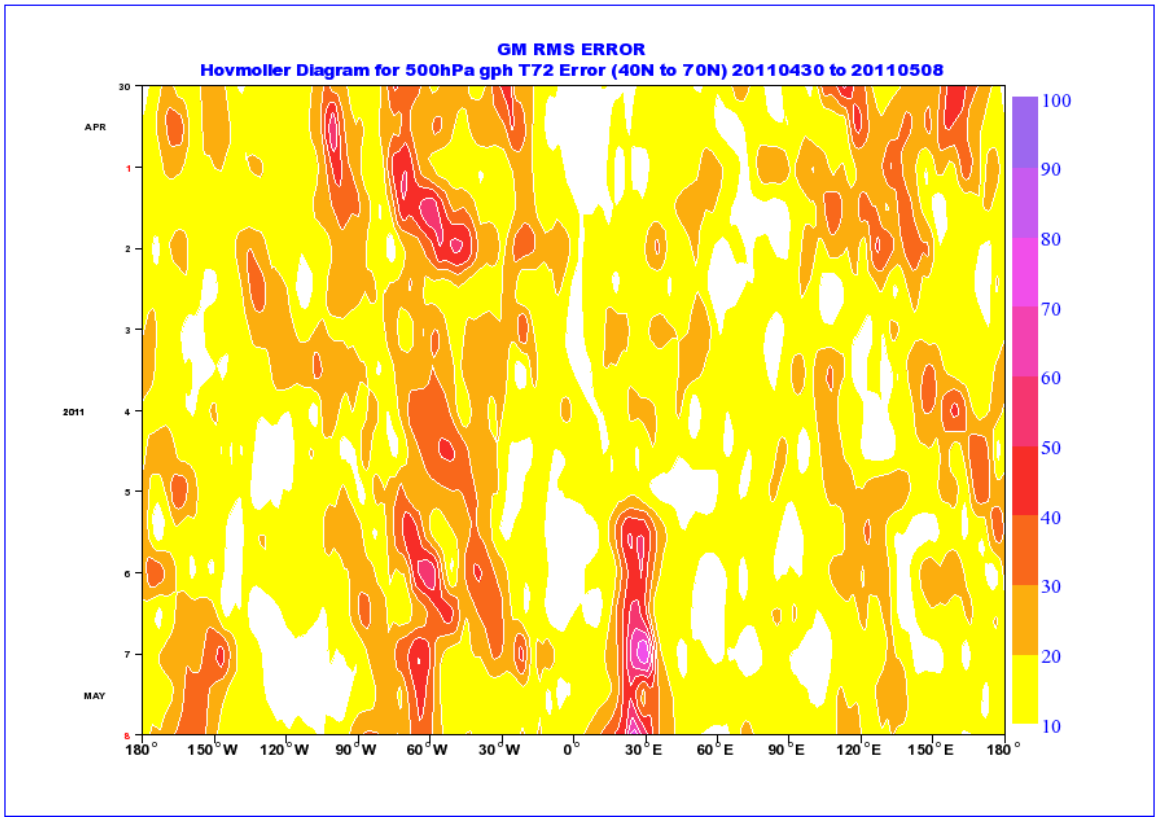

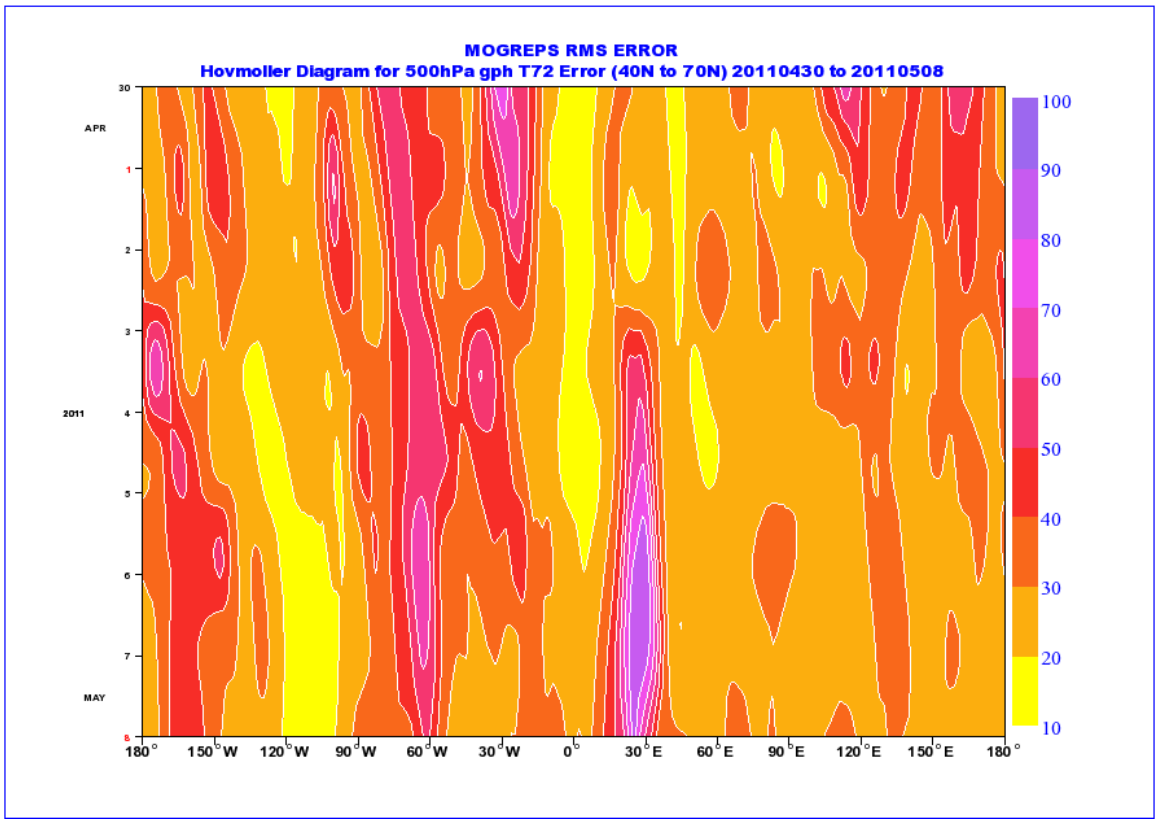

Figure 9 GM 500hPa gph Error versus Ensemble RMS Error, T+72.

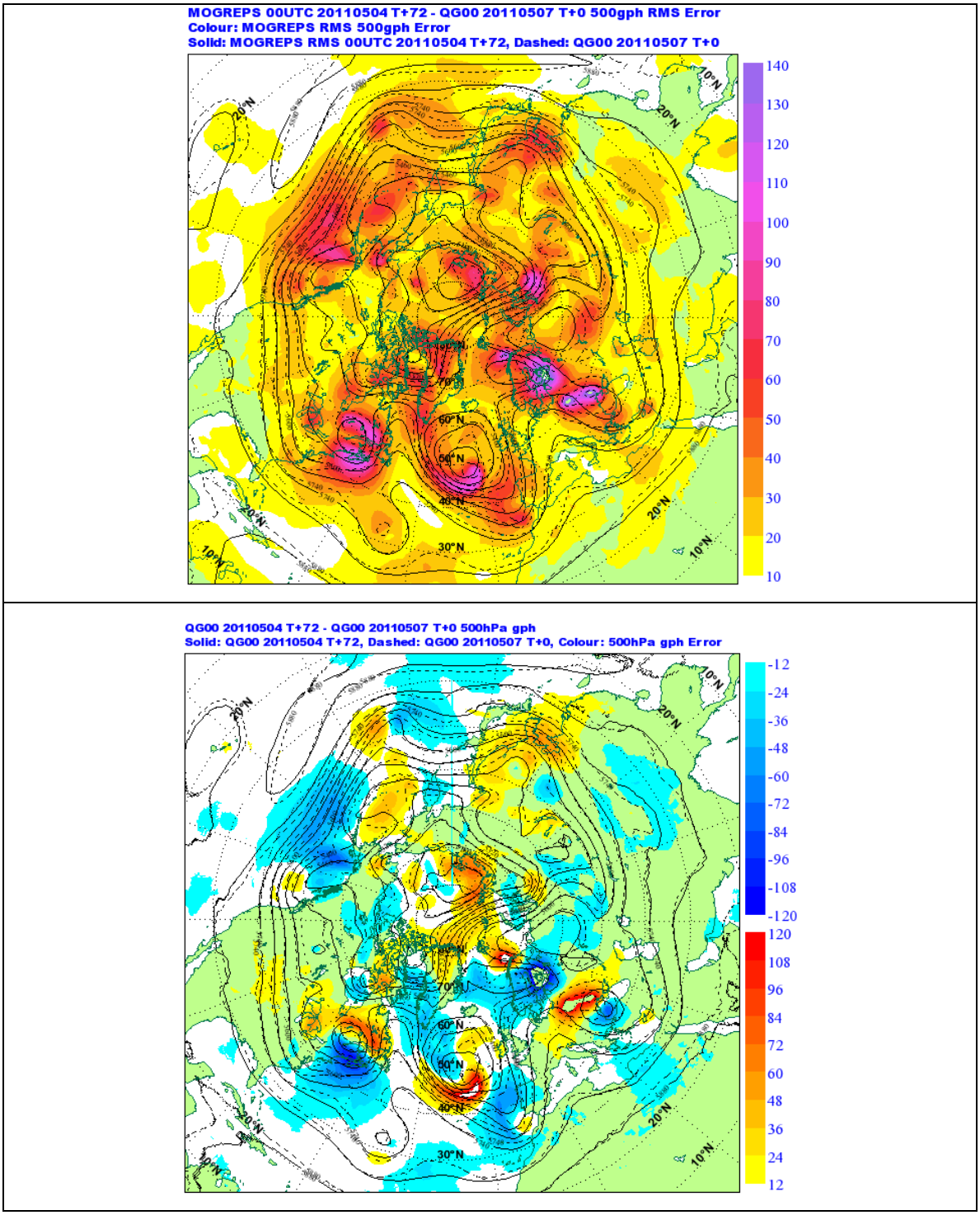

Figure 10 RMS Error of MOGREPS ensemble (top) and GM Error (lower) for the T+72 forecast verifying 7th May 2011. The large error identified through the Hovmöller treatment extending through the 3rd May to the 8th May, may be seen as associated with a trough disruption over eastern Europe.

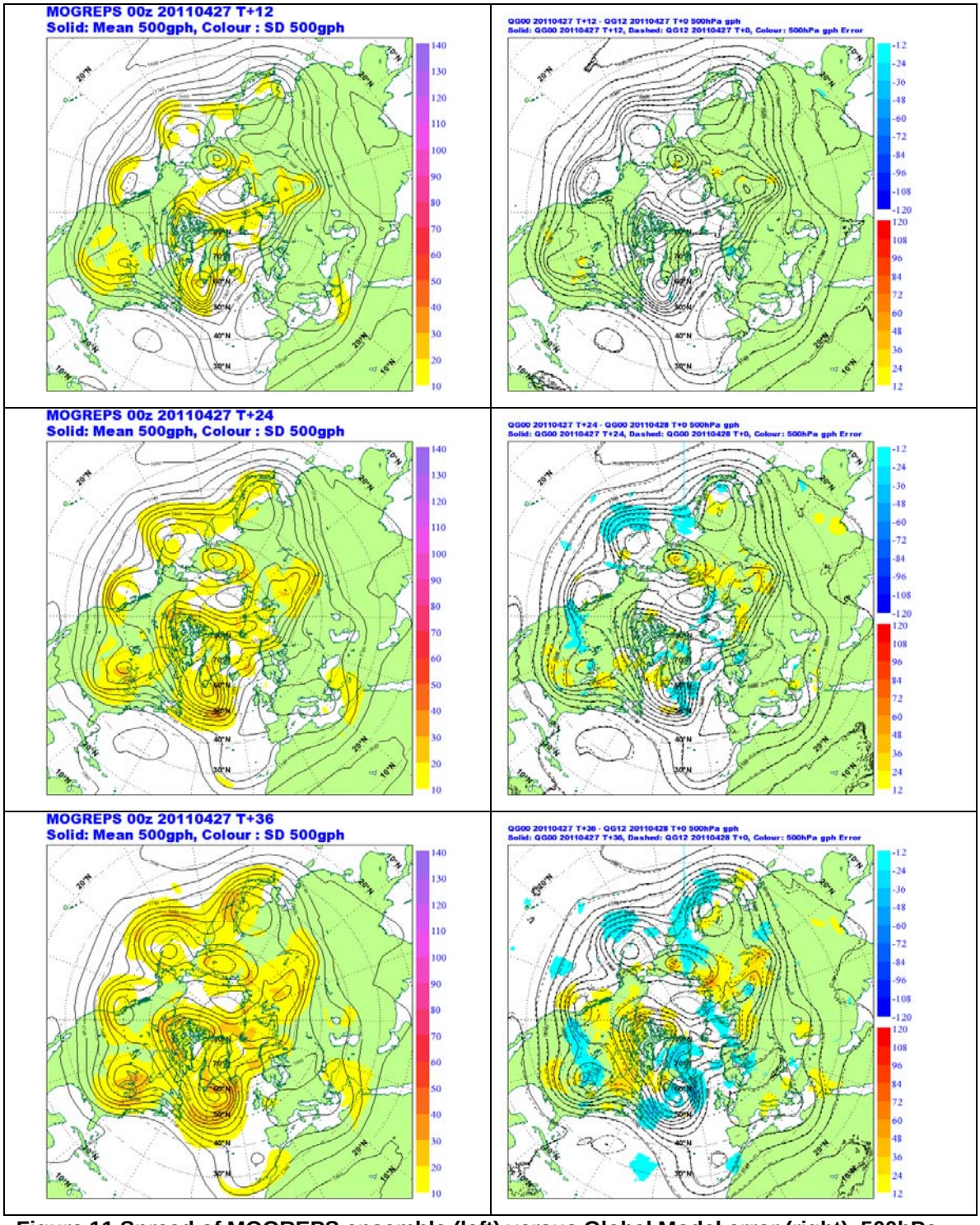

Figure 11 Spread of MOGREPS ensemble (left) versus Global Model error (right), 500hPa gph T+12 to T+36 for the Northern Hemisphere with forecast *data time* 00UTC 27th April 2011.

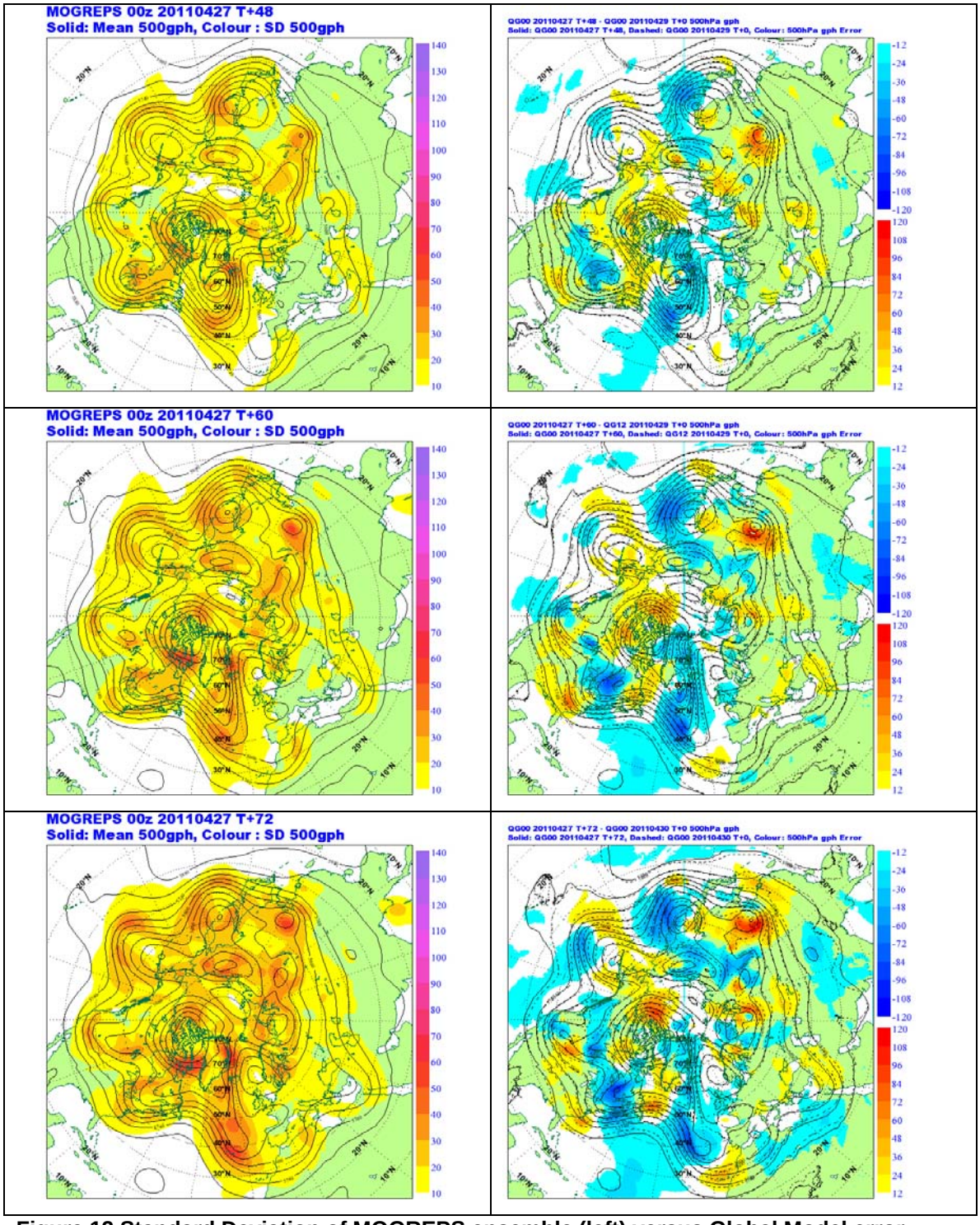

Figure 12 Standard Deviation of MOGREPS ensemble (left) versus Global Model error (right), 500hPa gph T+48 to T+72 for the Northern Hemisphere with forecast *data time* 00UTC 27th April 2011.

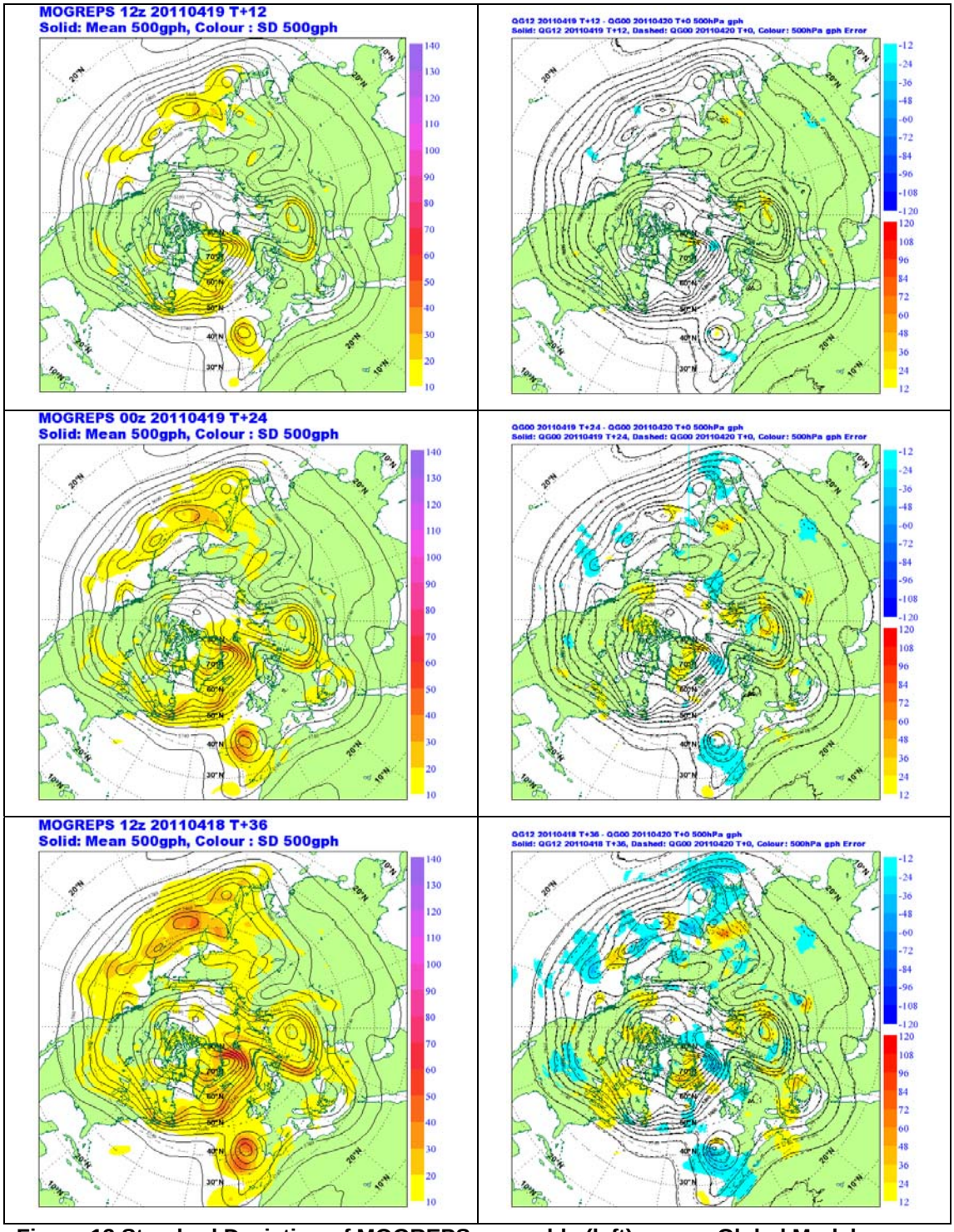

Figure 13 Standard Deviation of MOGREPS ensemble (left) versus Global Model error (right), 500hPa gph T+12 to T+36 for the Northern Hemisphere with forecast *verification time* 00UTC 20th April 2011.

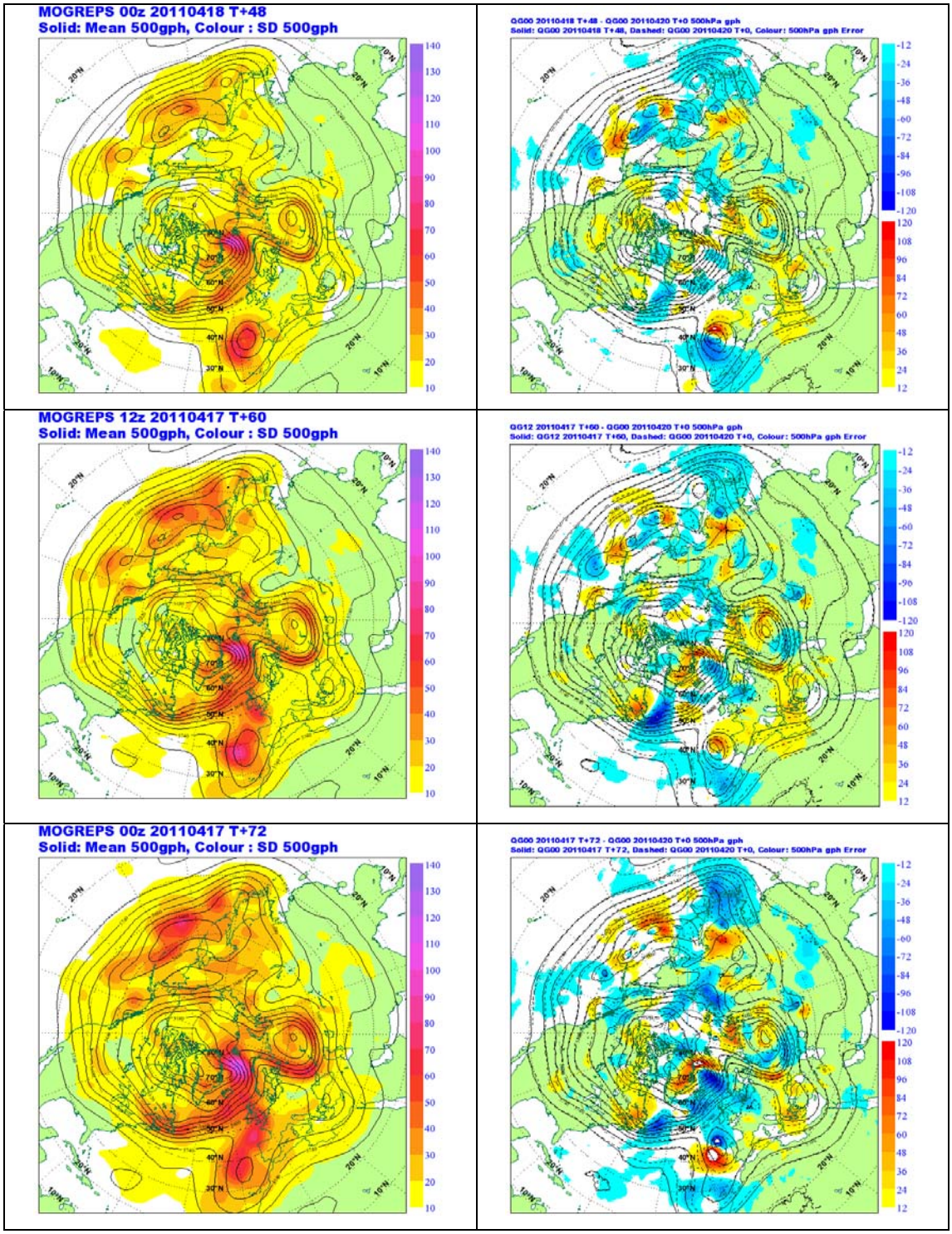

Figure 14 Standard Deviation of MOGREPS ensemble (left) versus Global Model error (right), 500hPa gph T+48 to T+72, for the Northern Hemisphere with forecast *verification time* 00UTC 20th April 2011.

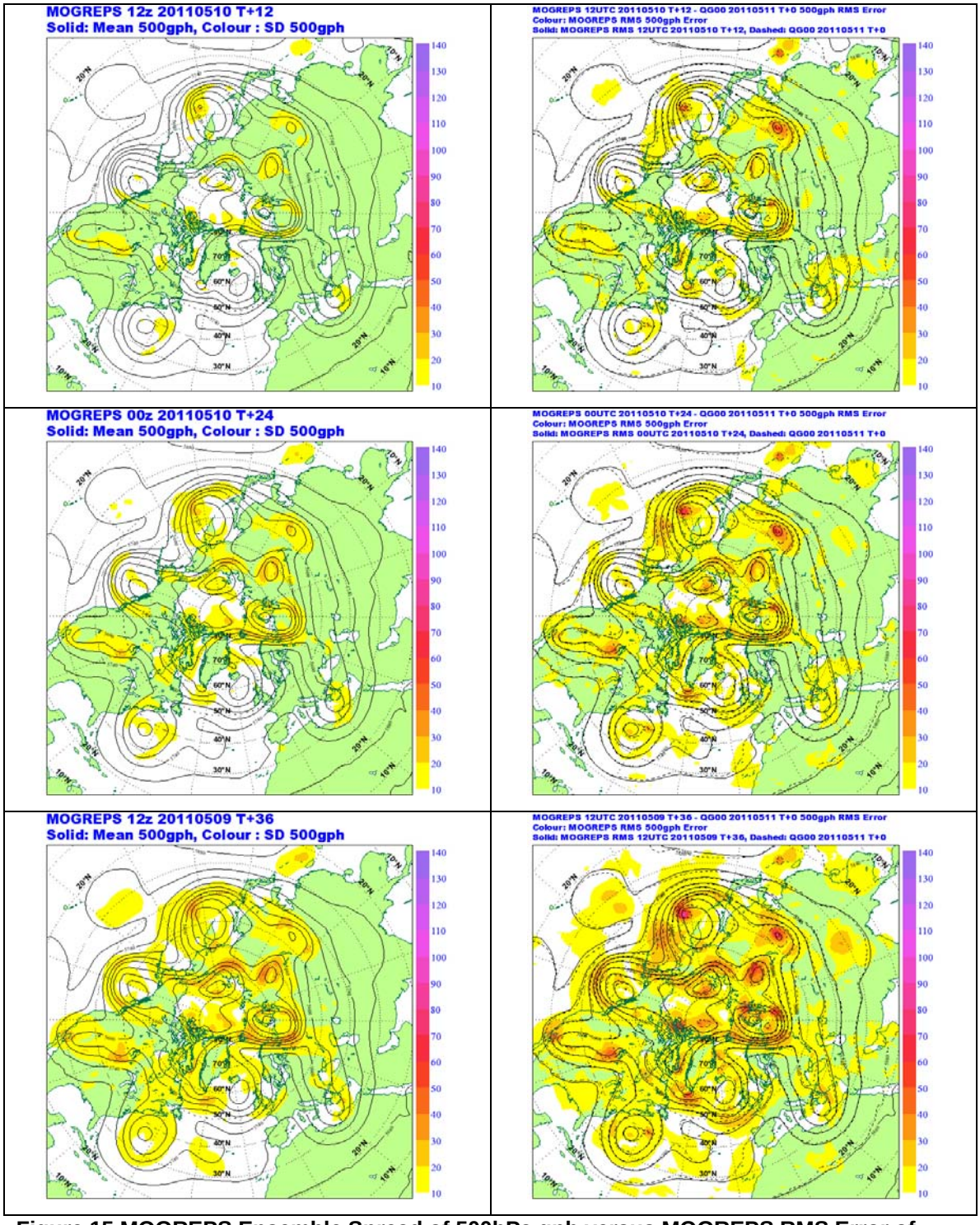

Figure 15 MOGREPS Ensemble Spread of 500hPa gph versus MOGREPS RMS Error of 500hPa gph, T+12 to T+36.

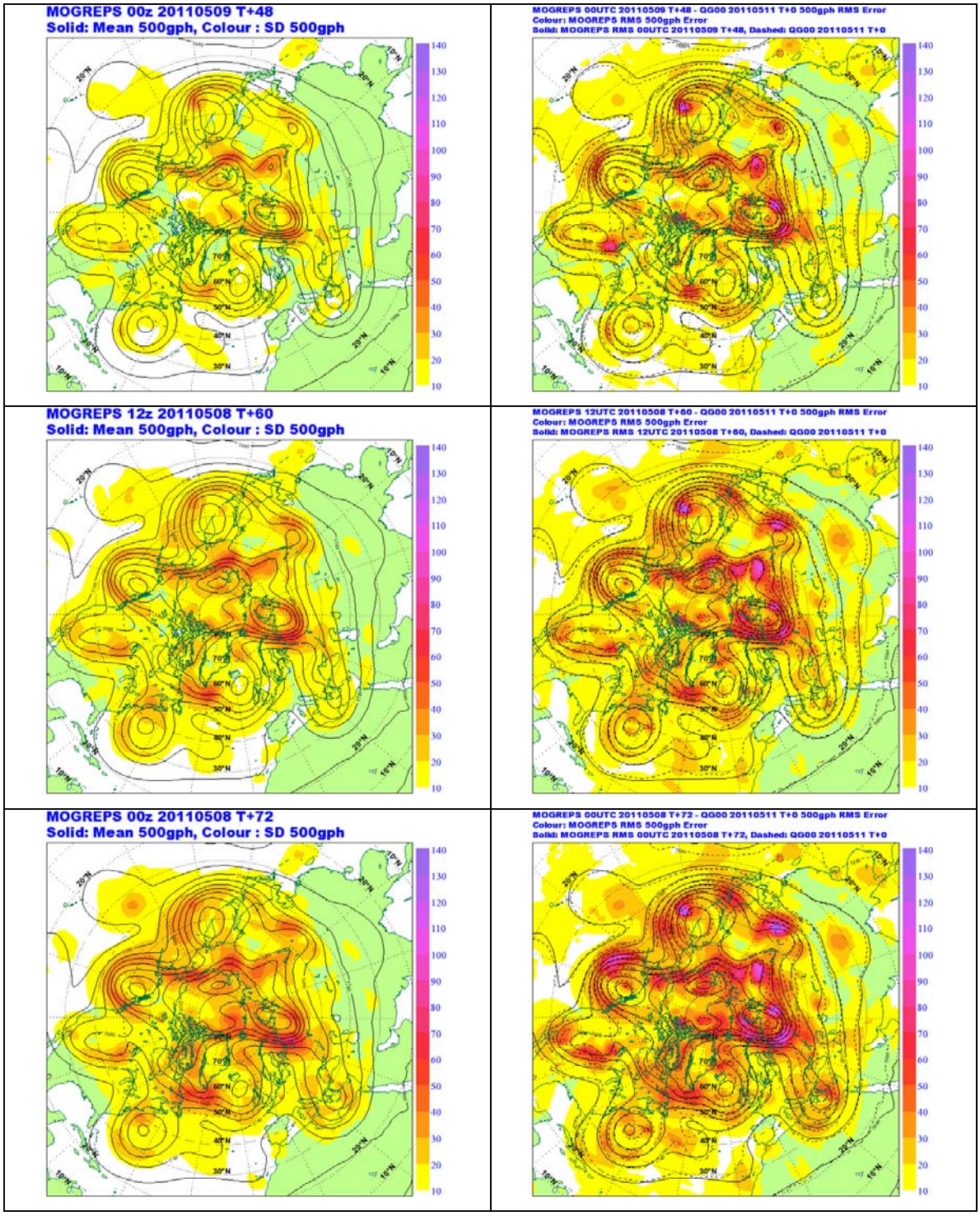

Figure 16 MOGREPS Ensemble Spread of 500hPa gph versus MOGREPS RMS Error of 500hPa gph, T+36 to T+72.

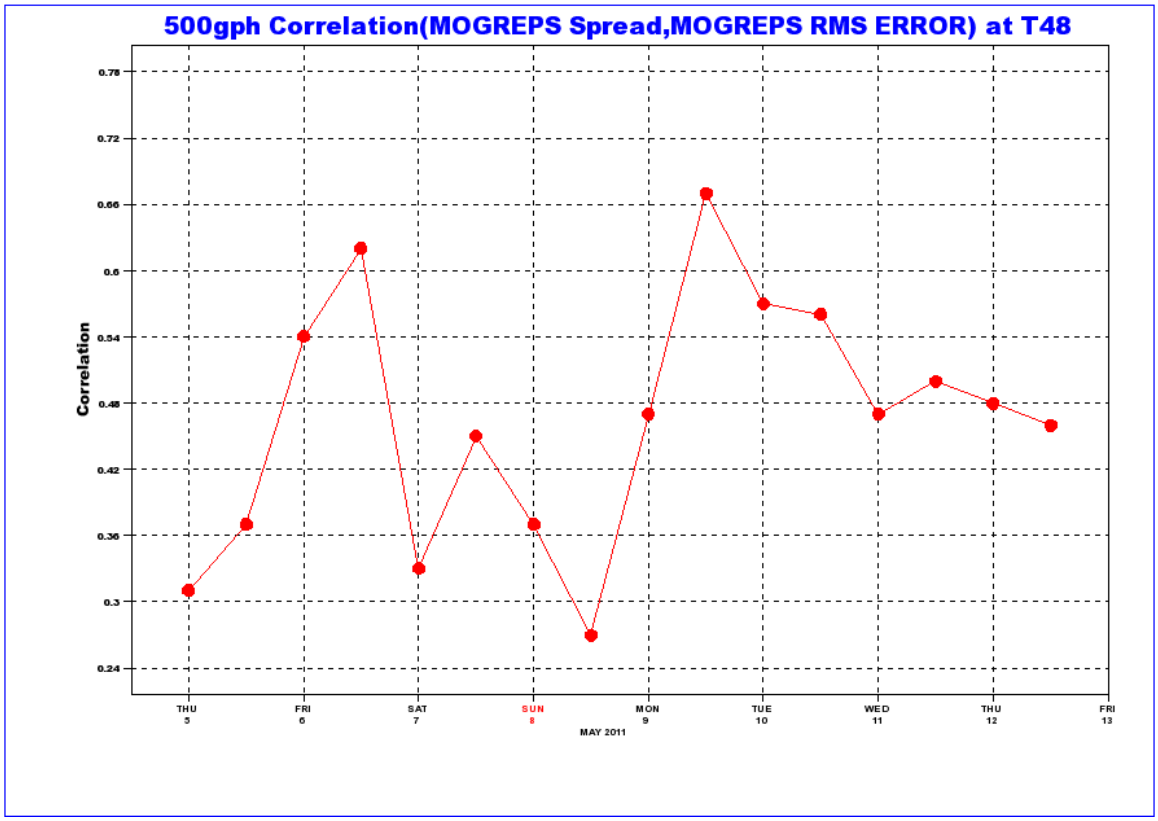

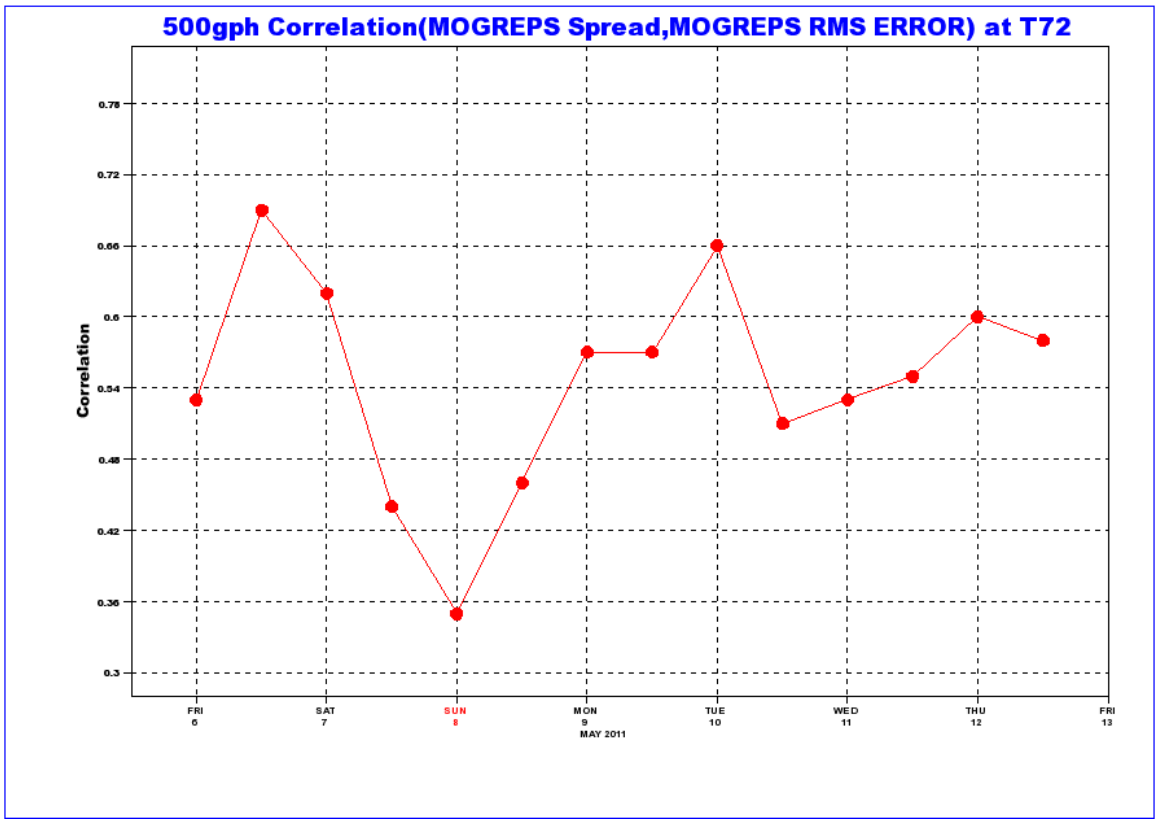

Figure 17 Correlation timeseries between MOGREPS spread and MOGREPS RMS Error at T+48 and T+72.

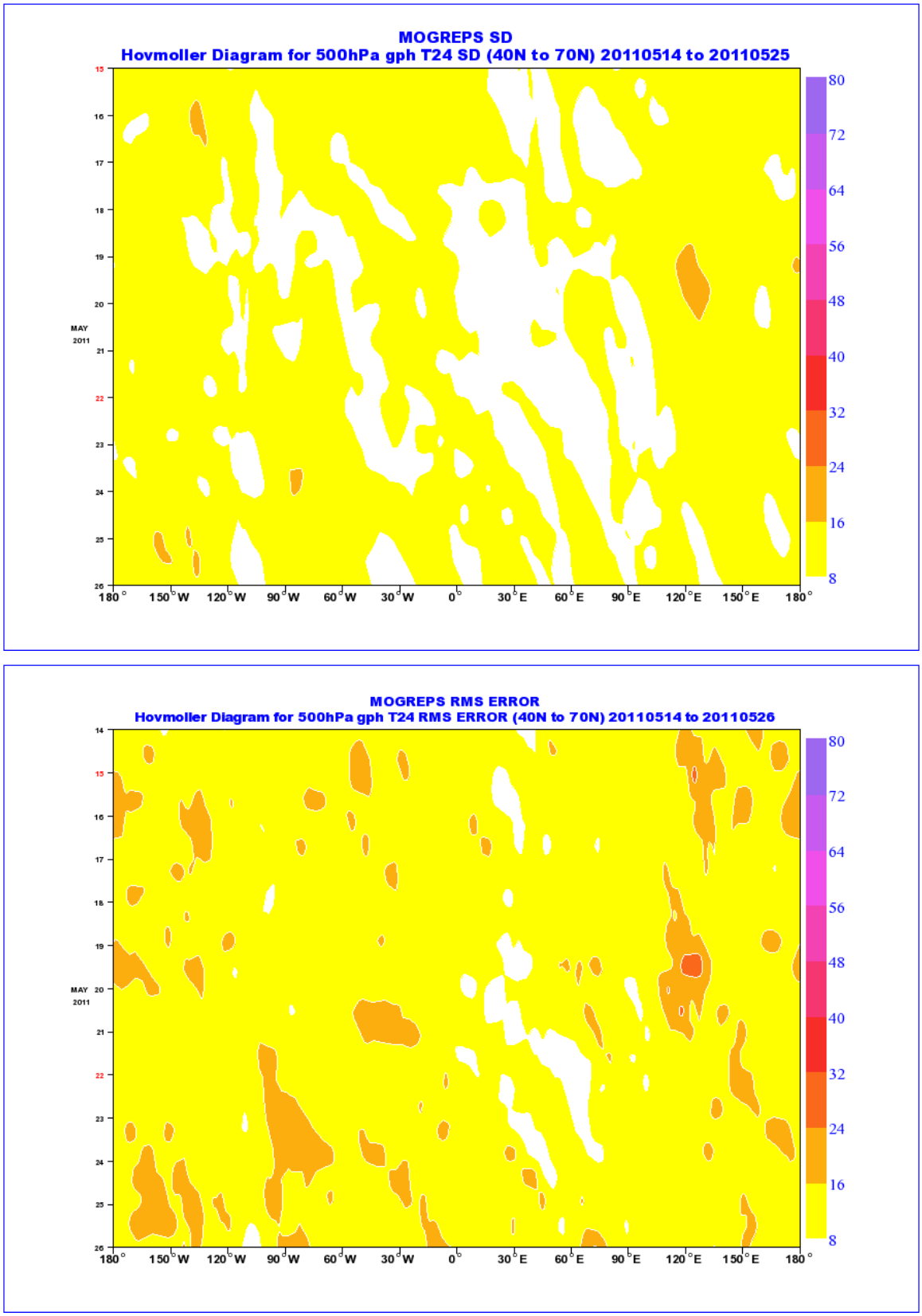

Figure 18 Hovmöller Diagrams of MOGREPS Standard Deviation versus RMS Error at T+24 with latitudinal mean across 40N to 70N.

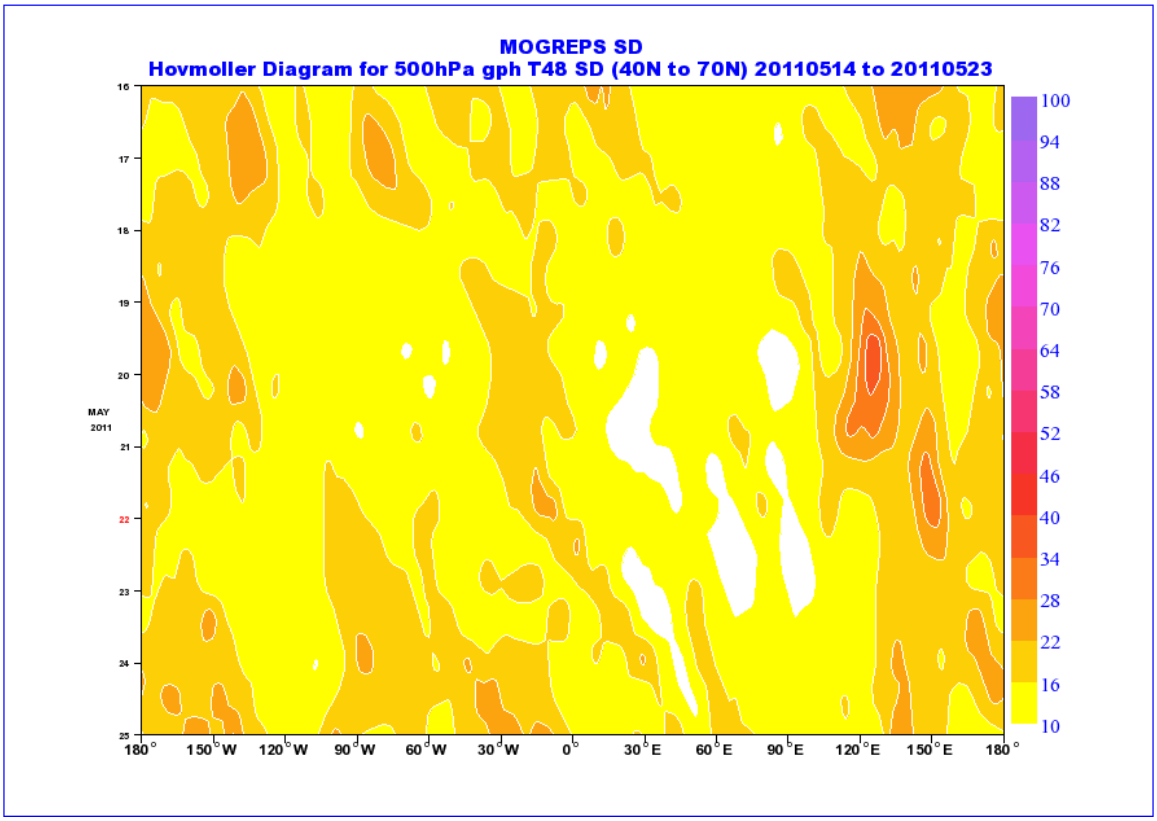

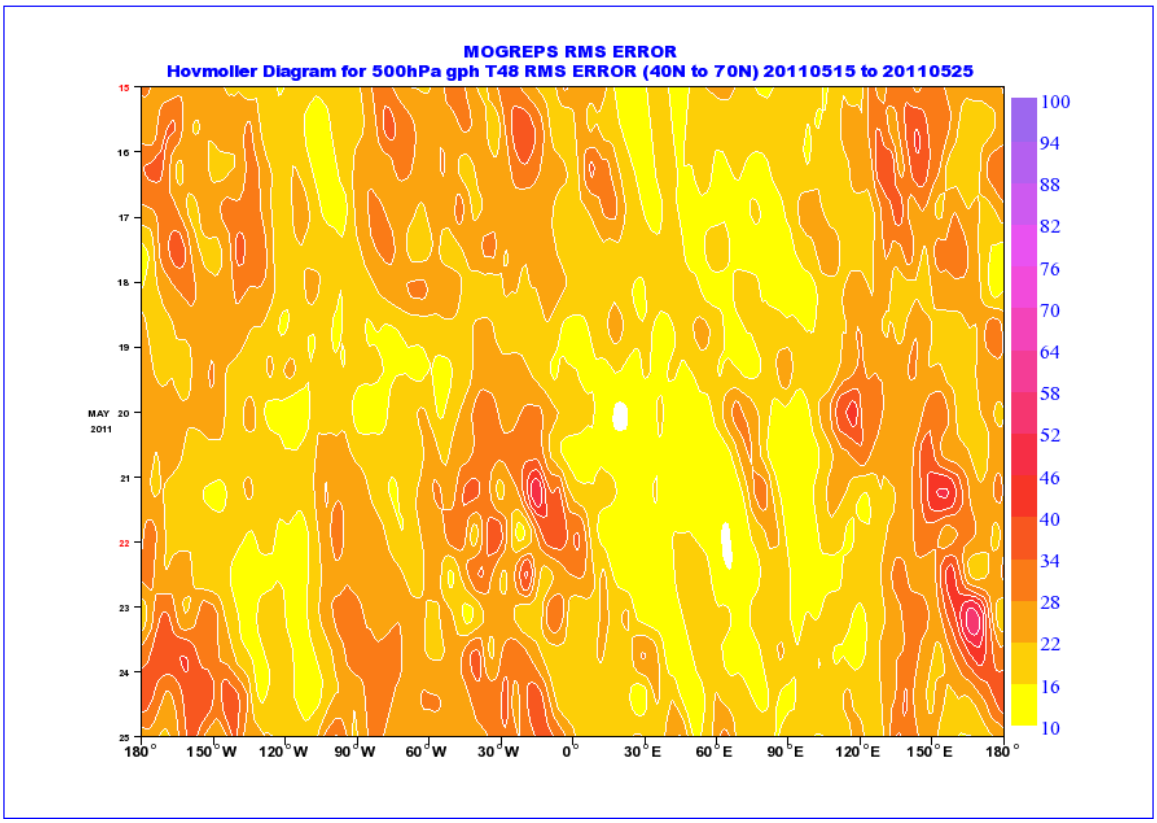

Figure 19 Hovmöller Diagrams of MOGREPS Standard Deviation versus RMS Error at T+48 with latitudinal mean across 40N to 70N.

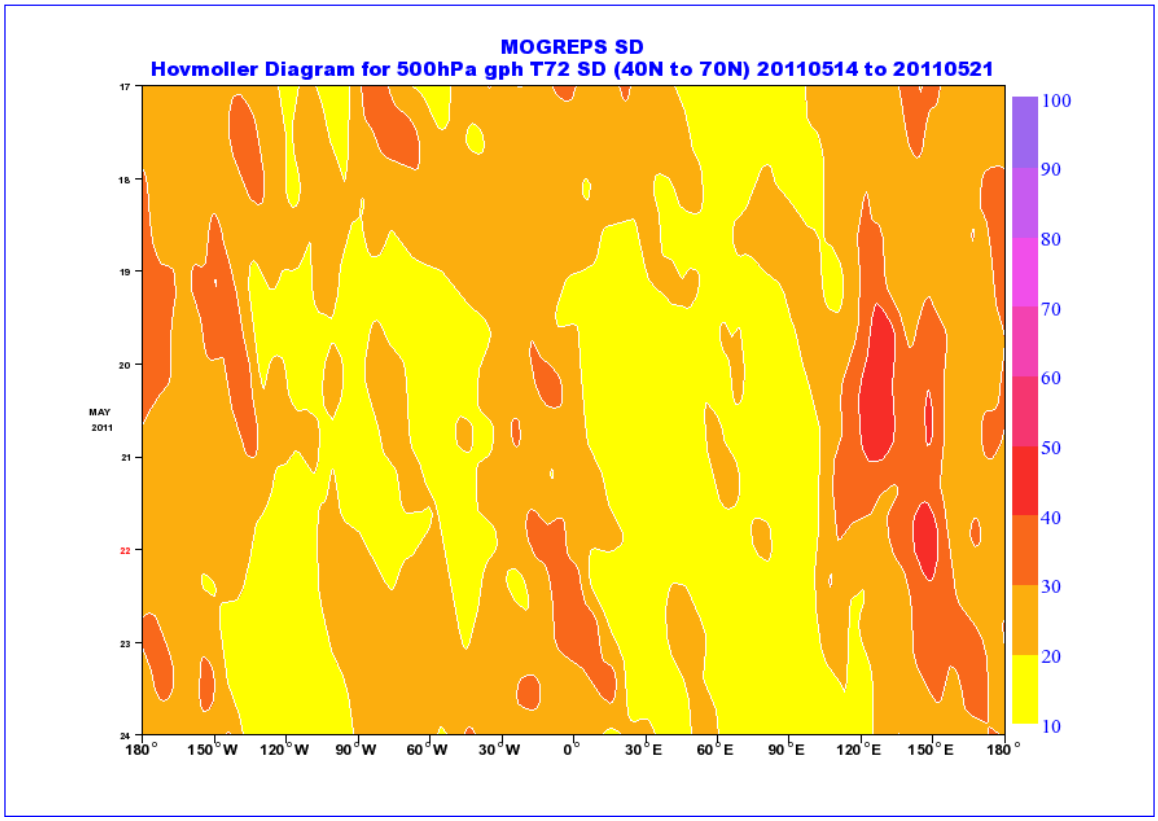

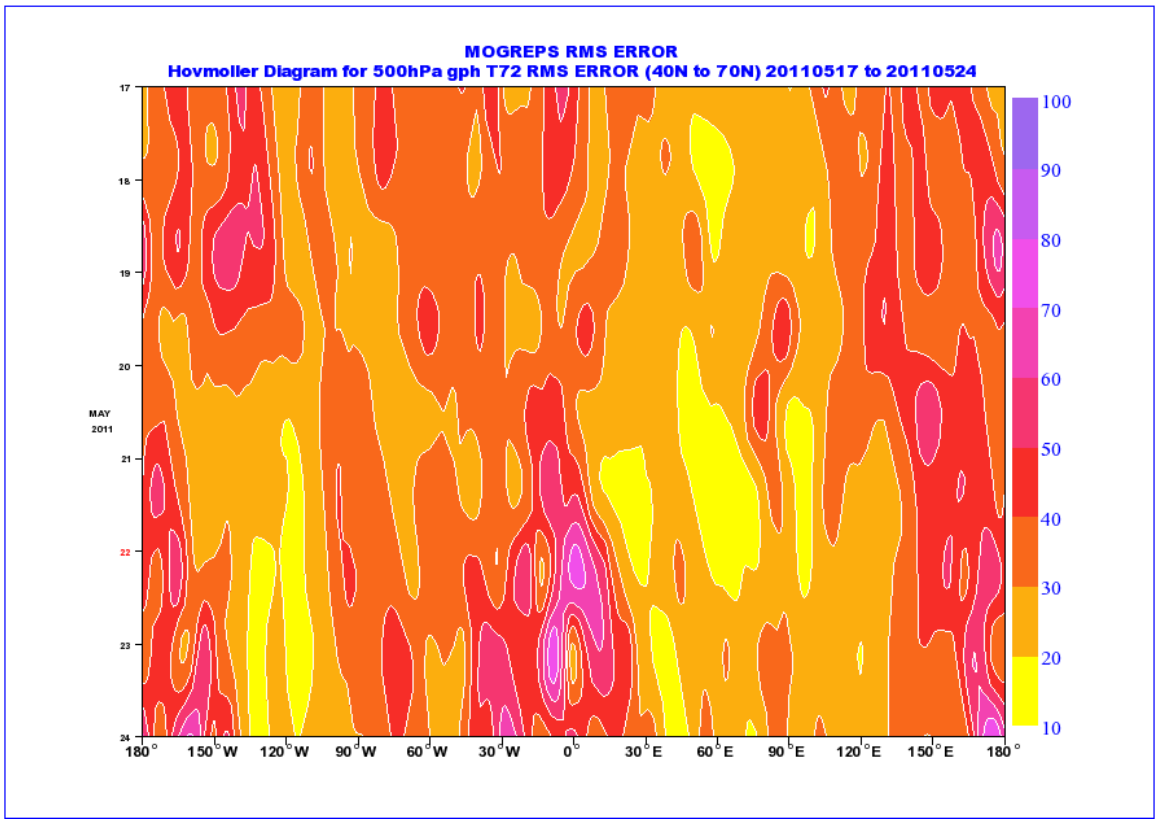

Figure 20 Hovmöller Diagrams of MOGREPS Standard Deviation versus RMS Error at T+72 with latitudinal mean across 40N to 70N.

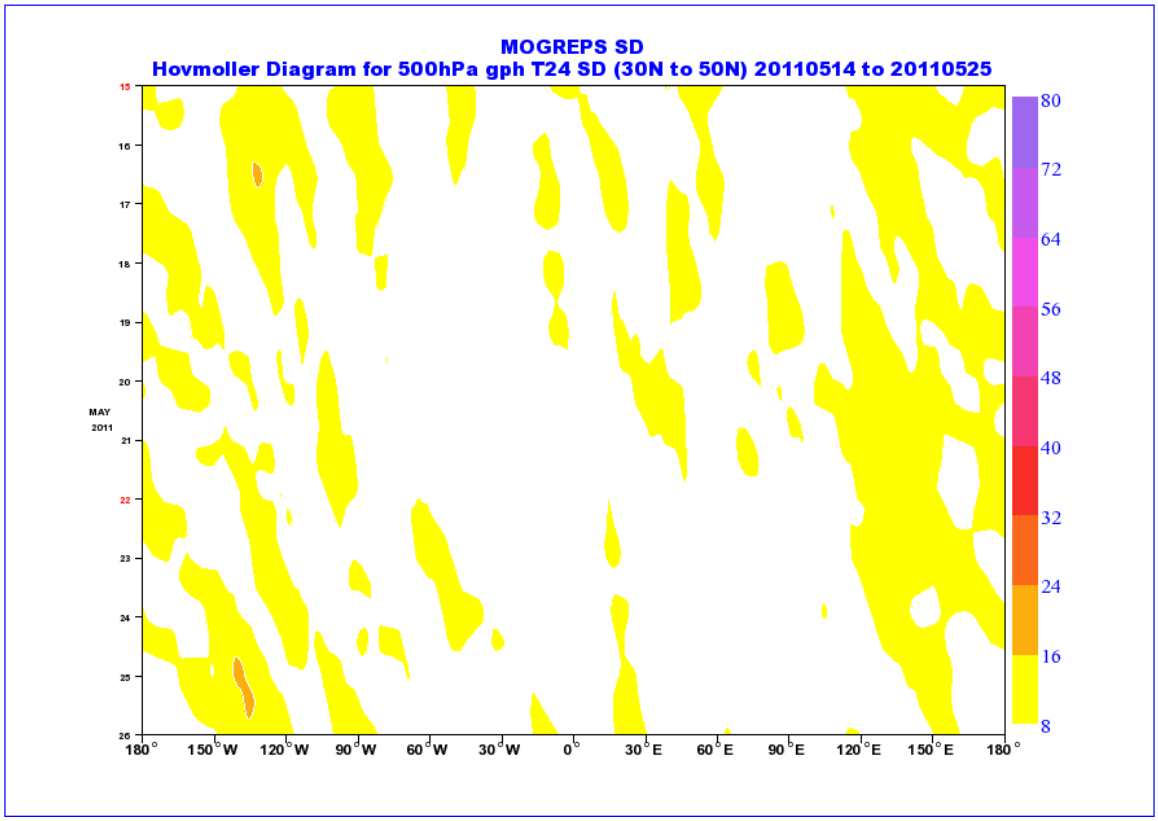

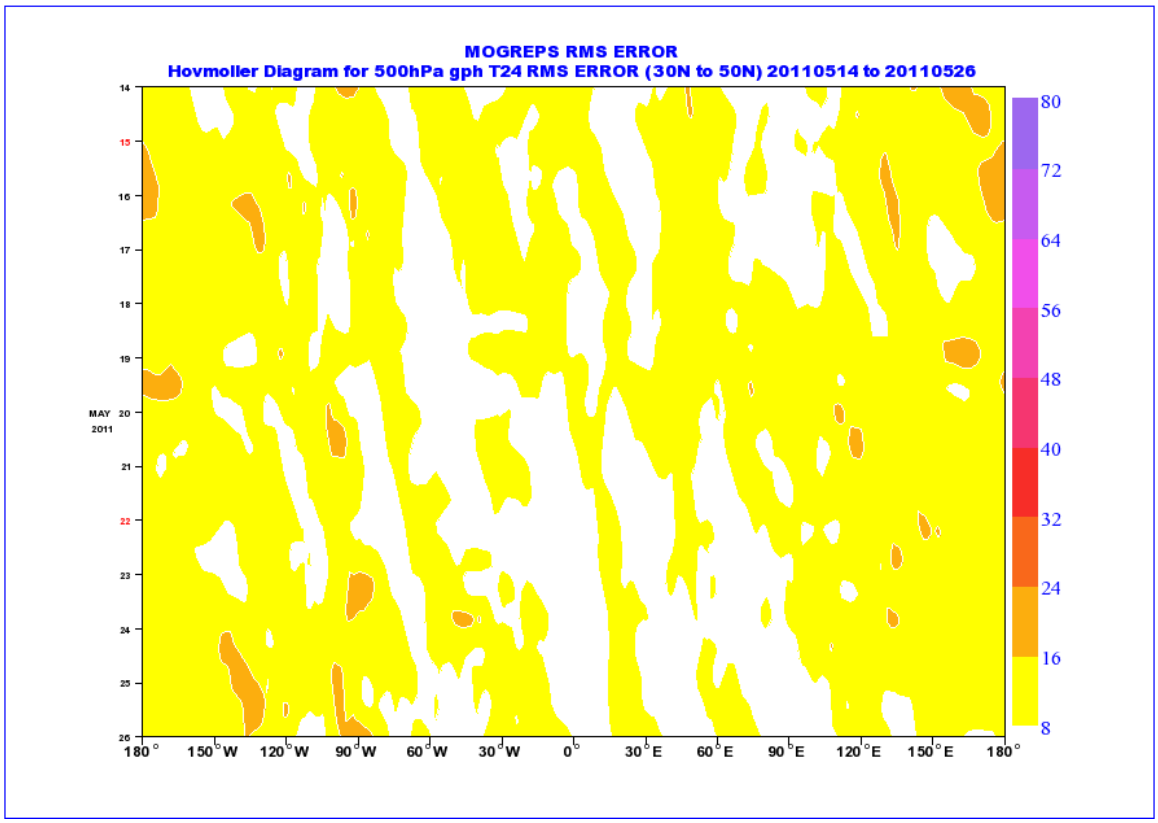

Figure 21 Hovmöller Diagrams of MOGREPS Standard Deviation versus RMS Error at T+24 with latitudinal mean across 30N to 50N.

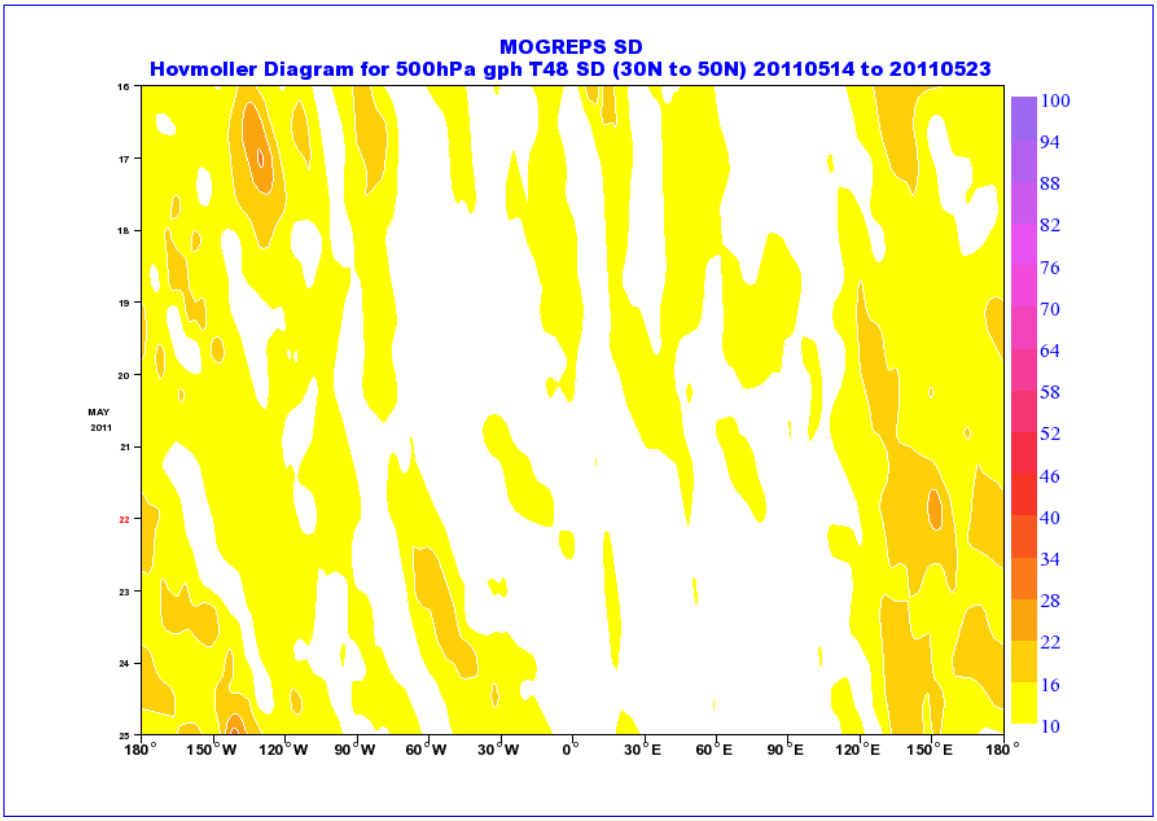

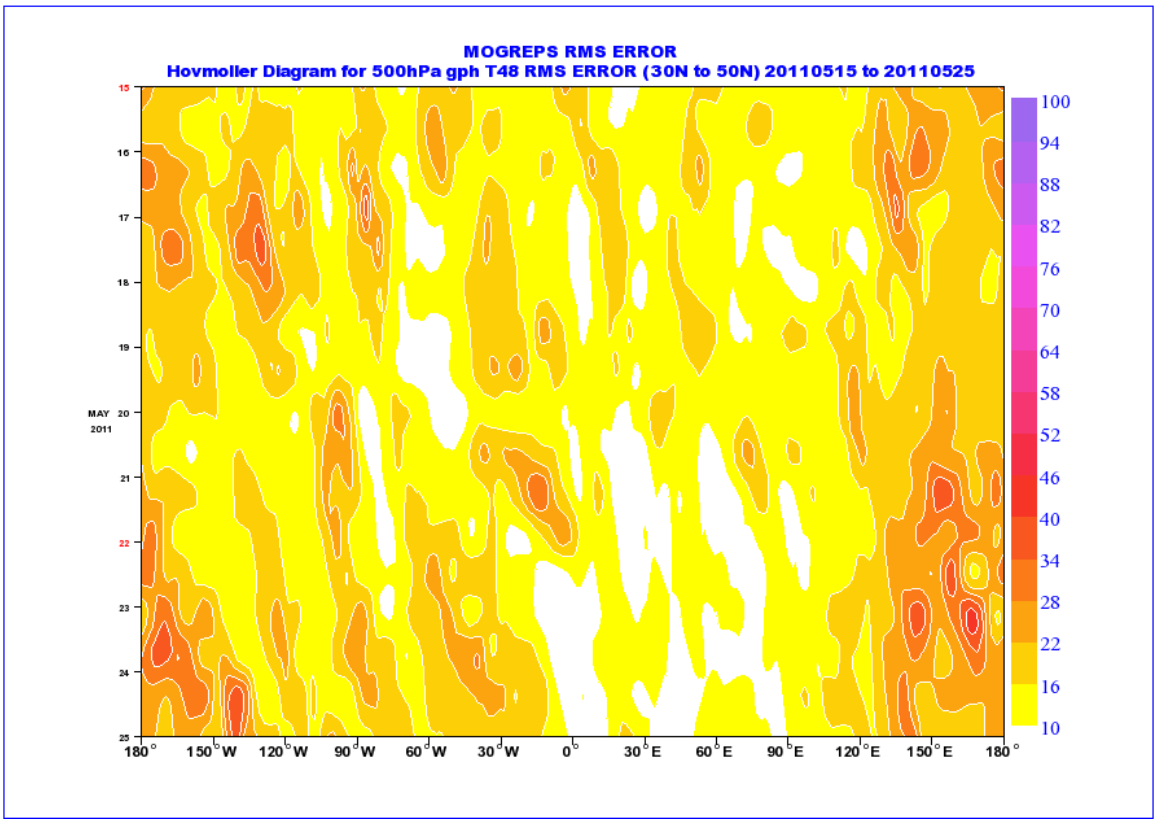

Figure 22 Hovmöller Diagrams of MOGREPS Standard Deviation versus RMS Error at T+48 with latitudinal mean across 30N to 50N.

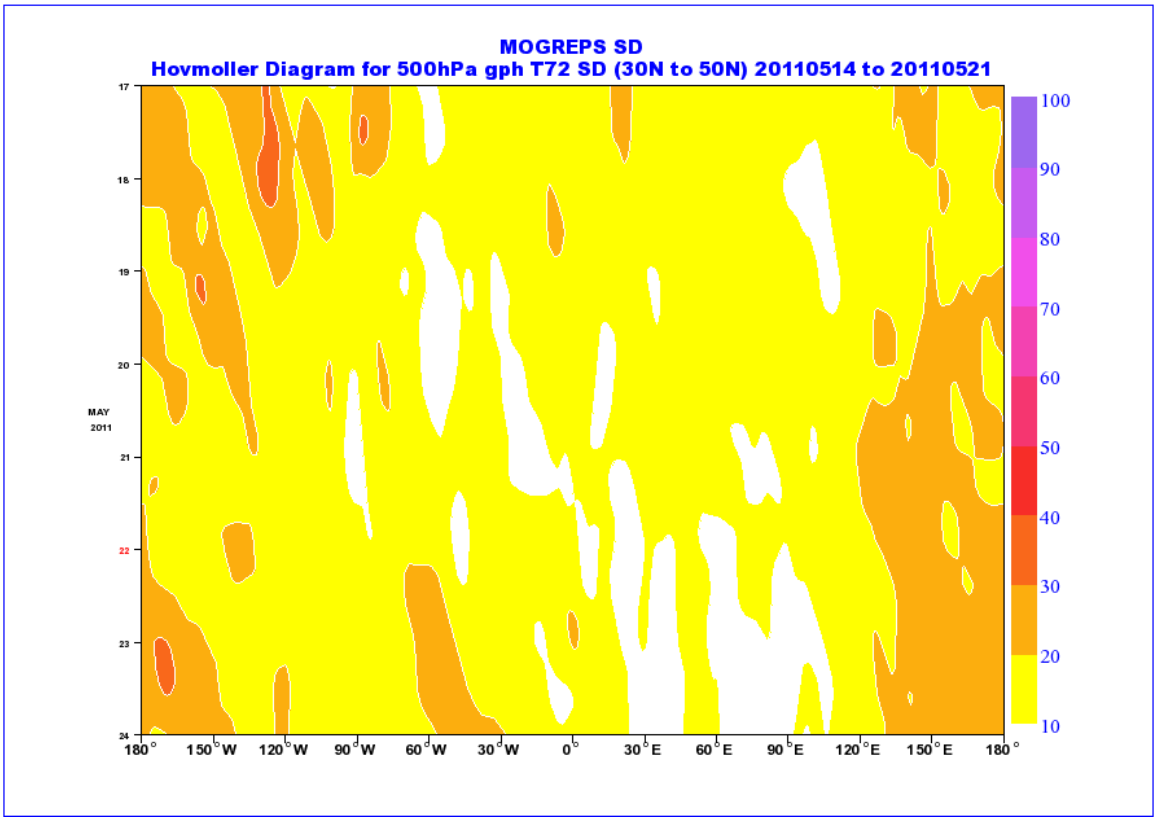

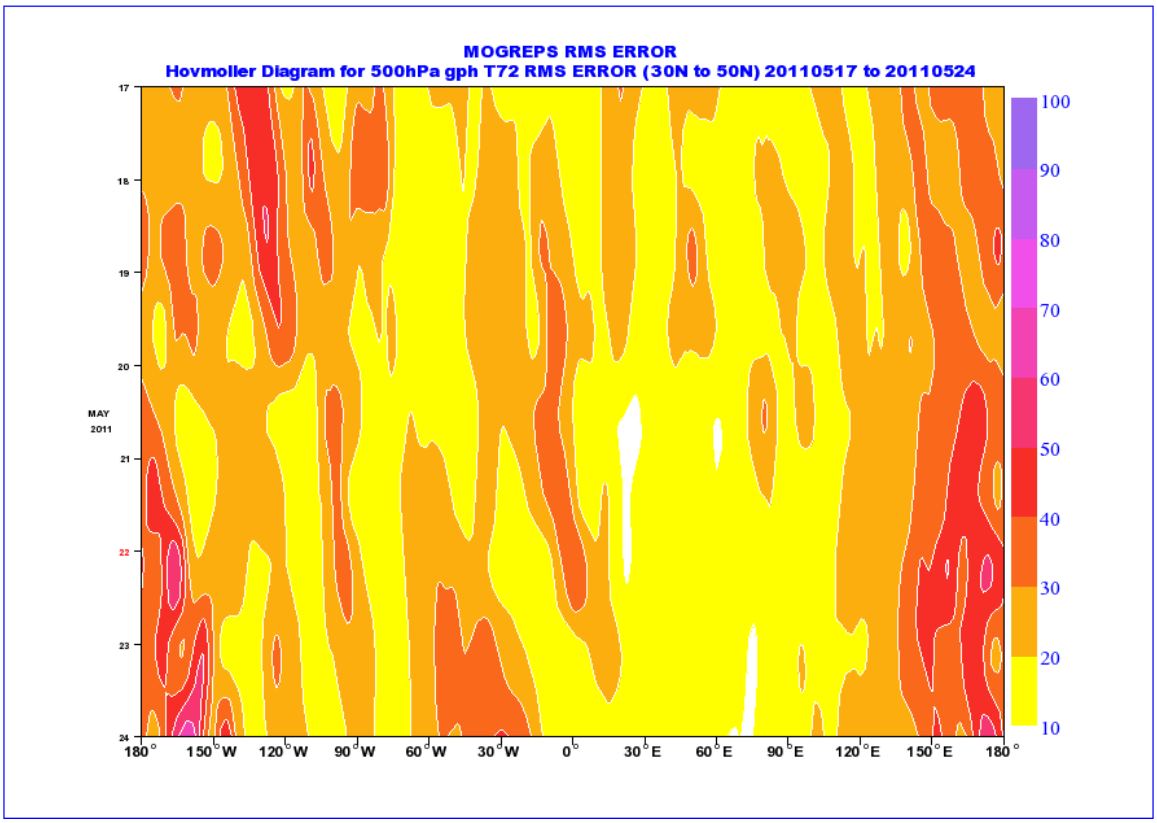

Figure 23 Hovmöller Diagrams of MOGREPS Standard Deviation versus RMS Error at T+72 with latitudinal mean across 30N to 50N.

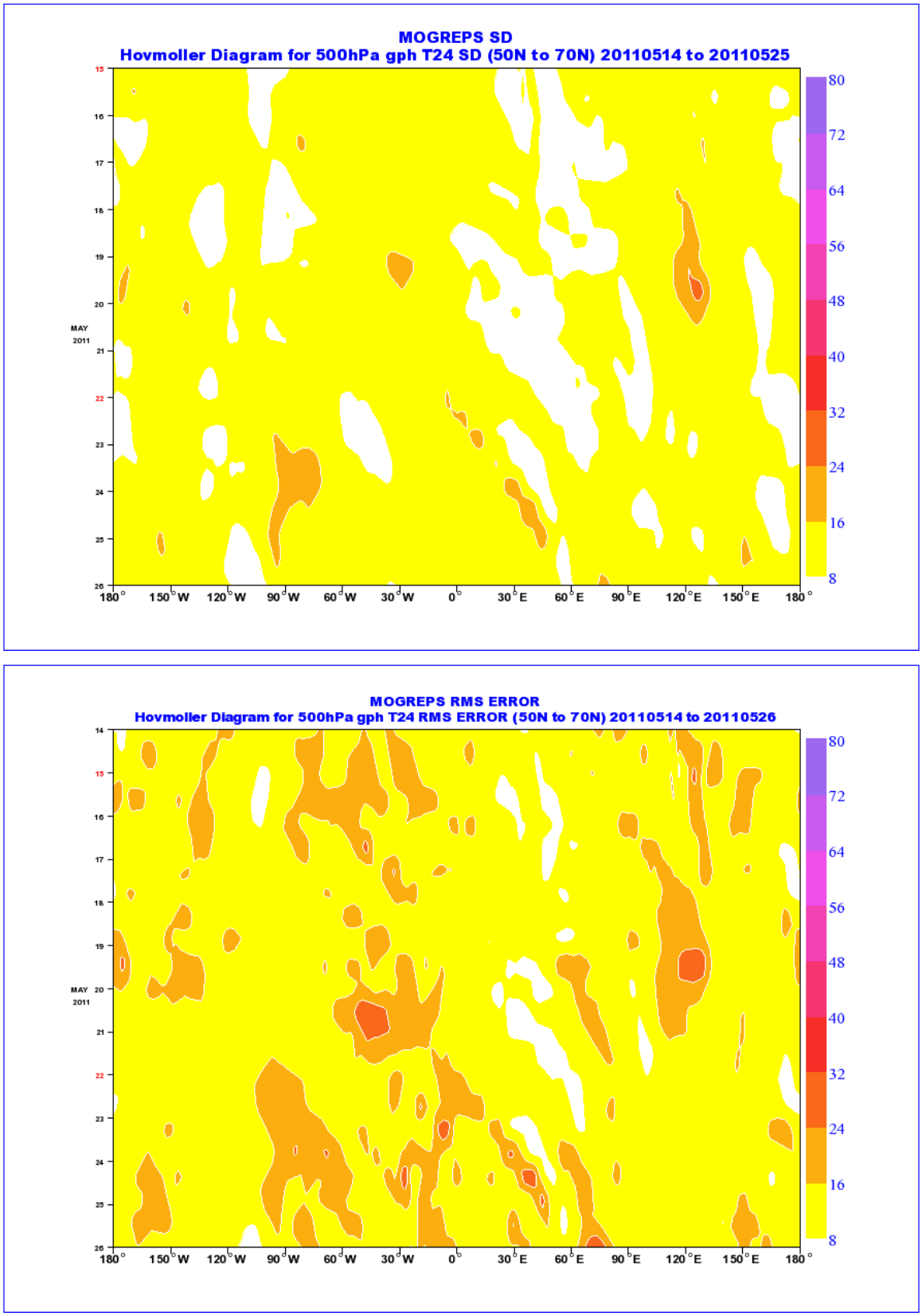

Figure 24 Hovmöller Diagrams of MOGREPS Standard Deviation versus RMS Error at T+24 with latitudinal mean across 50N to 70N.

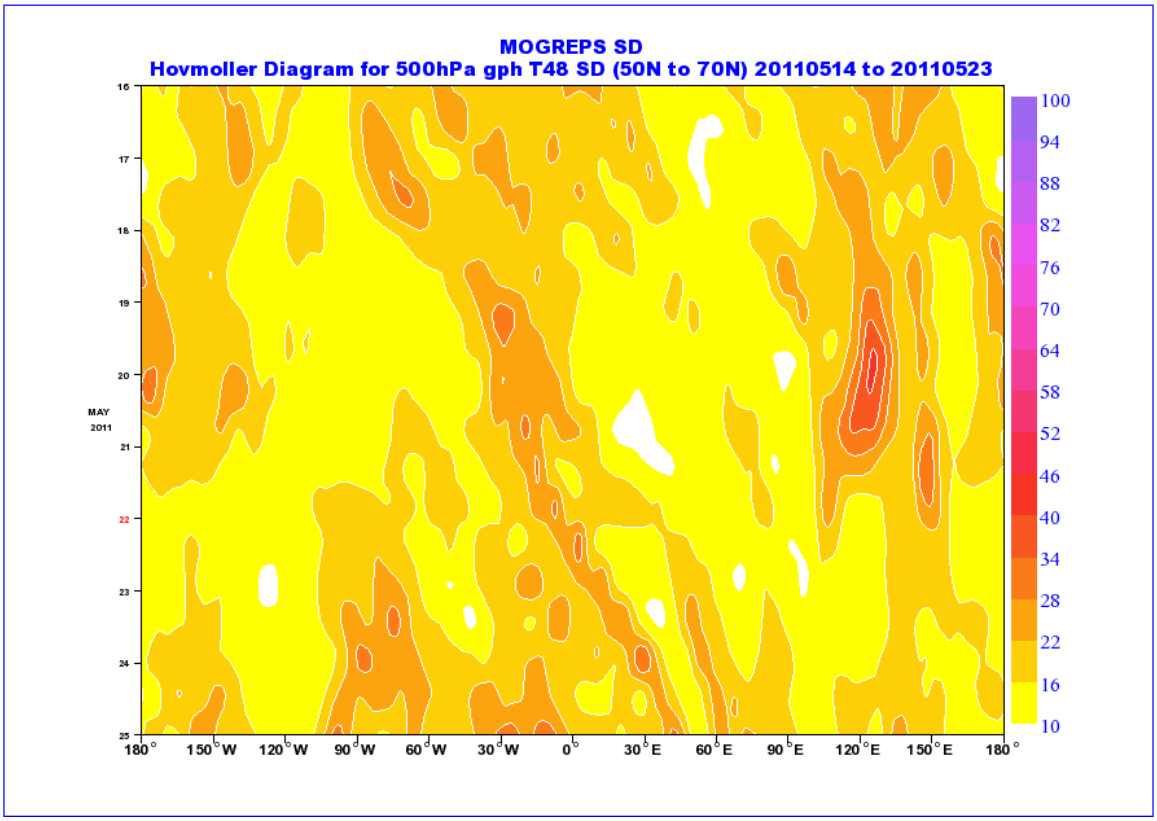

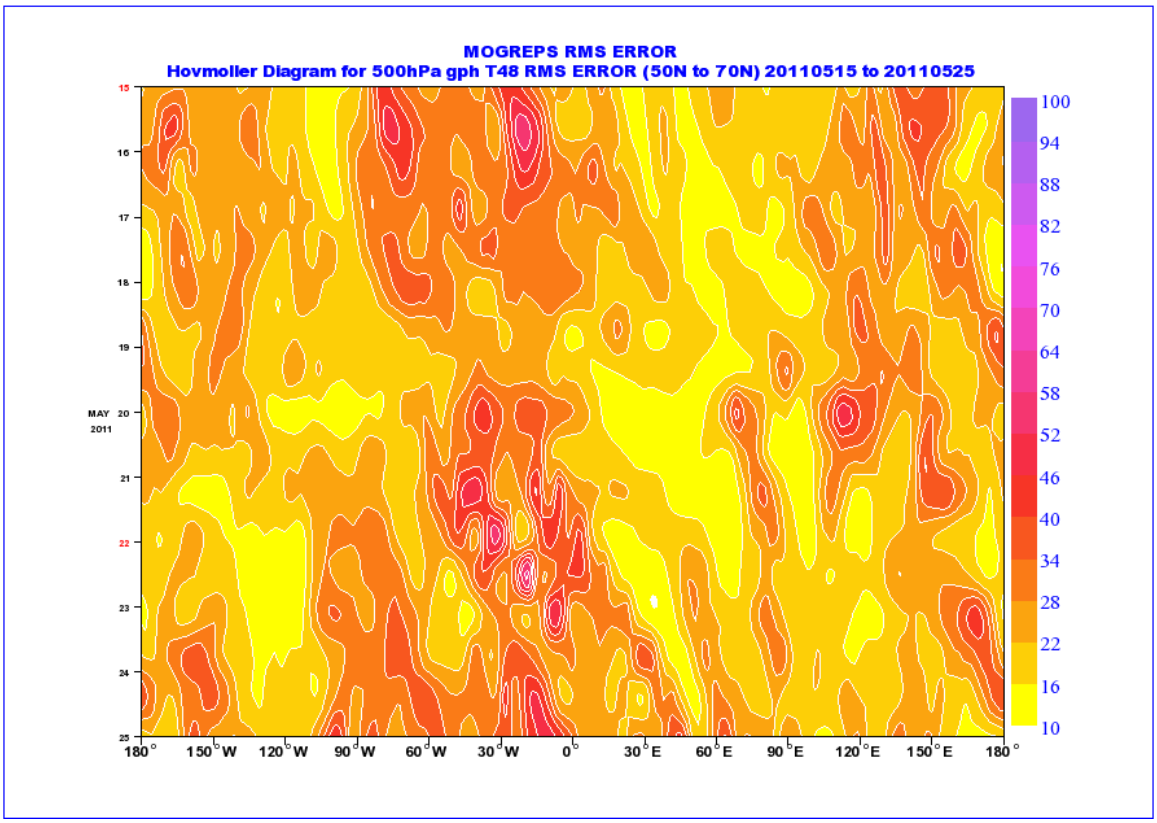

Figure 25 Hovmöller Diagrams of MOGREPS Standard Deviation versus RMS Error at T+48 with latitudinal mean across 50N to 70N.

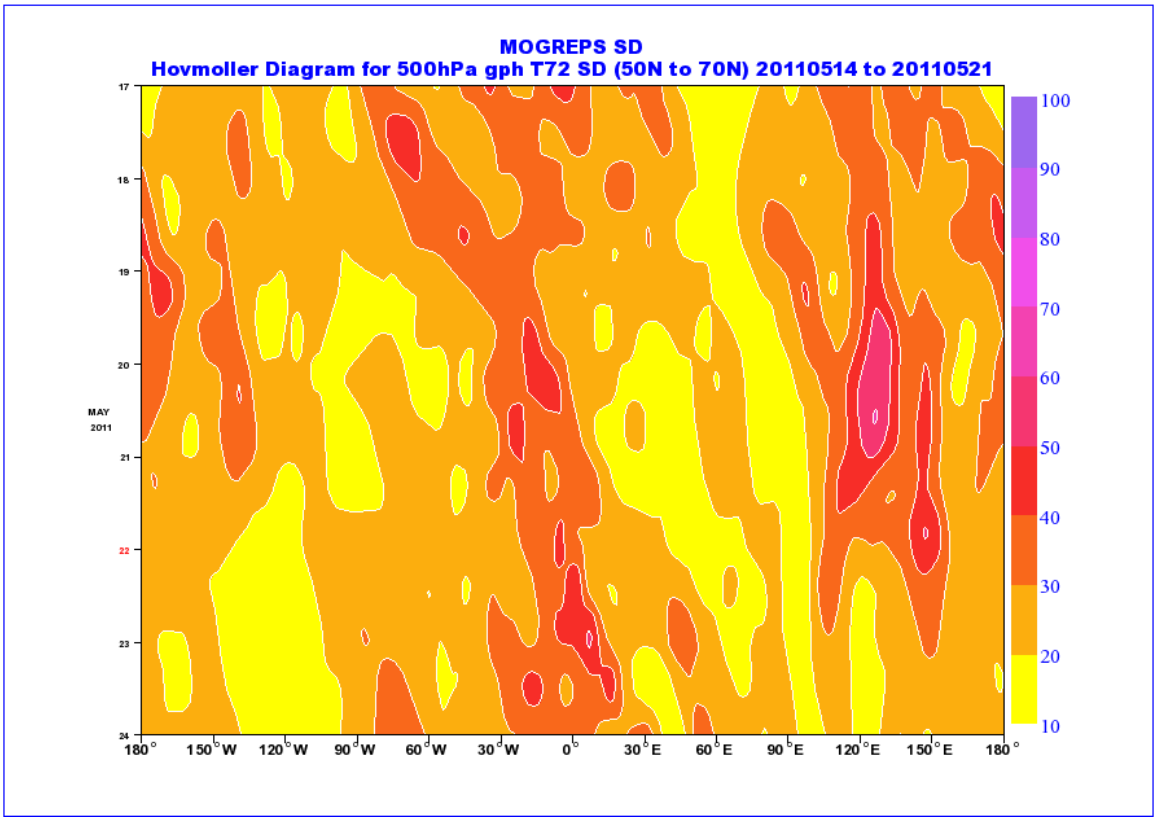

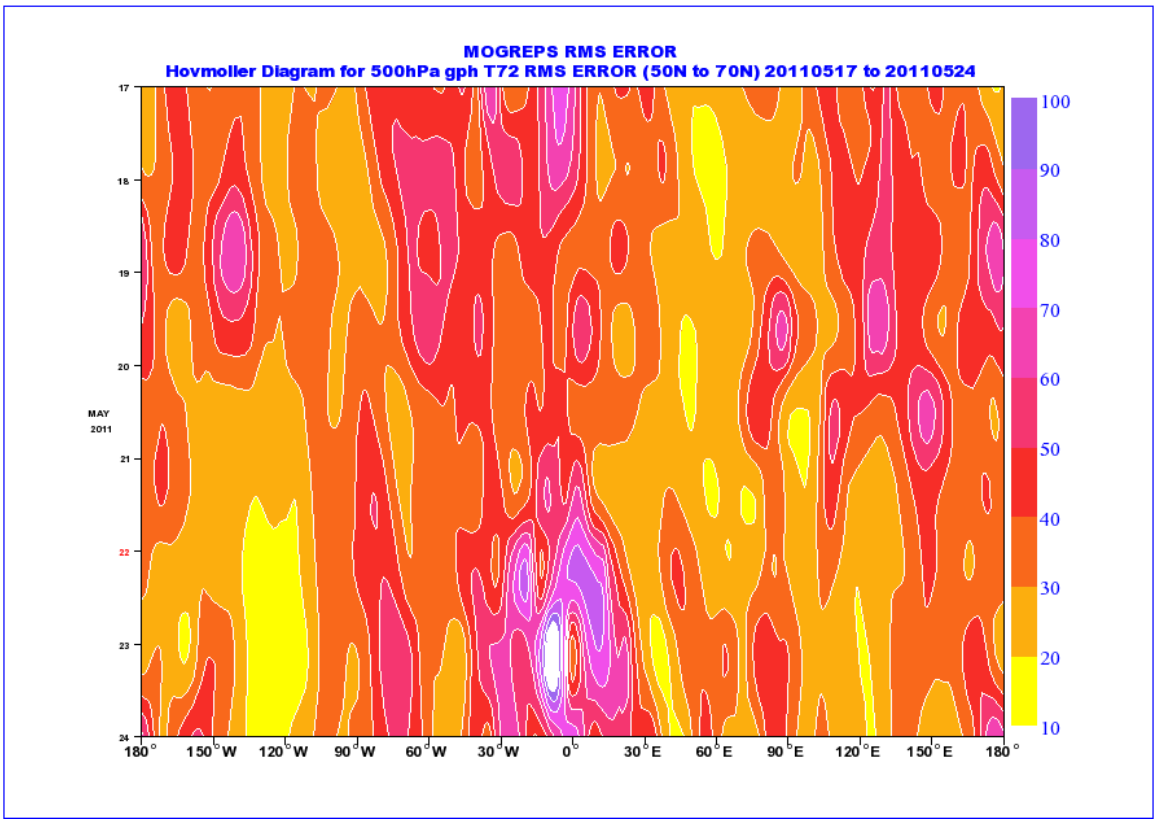

Figure 26 Hovmöller Diagrams of MOGREPS Standard Deviation versus RMS Error at T+72 with latitudinal mean across 50N to 70N.

Met Office
FitzRoy Road, Exeter
Devon EX1 3PB
United Kingdom

Tel: 0870 900 0100
Fax: 0870 900 5050
enquiries@metoffice.gov.uk
www.metoffice.gov.uk